Energy & Buildings 253 (2021) 111504

Contents lists available at ScienceDirect

Energy & Buildings

journal homepage: www.elsevier.com/locate/enb

A new HVAC ductwork steady-state flow analysis method: The Minimum Energy Dissipation Principle applied to flow networks including the effects of branched junctions

Víctor-Manuel Soto-Francés [a,*], José-Manuel Pinazo-Ojer [a], Emilio-José Sarabia-Escrivá [a], Joaquin Navarro-Esbrí [b]

[a] Dpto. Termodinamica Aplicada, Universitat Polite'cnica de Vale'ncia, Edificio 5J. ETSII. C/Camino de Vera S/n, 46022 Valencia, Spain
[b] ISTENER Research Group, Dept. of Mechanical Engineering and Construction, Universitat Jaume I, Campus de Riu Sec s/n, E12071 Castell de la Plana, Spain

ARTICLE INFO

Article history:
Received 13 May 2021
Revised 2 September 2021
Accepted 21 September 2021
Available online 23 September 2021

Keywords:
Minimum Energy Dissipation Principle
Steady-state flow
Ductwork
HVAC
T-junction
Junction dominated flows

ABSTRACT

The fact that the popular head loss coefficient concept, may become negative in branched junctions, is a symptom that something is not correctly managed. The paper makes a review of recent works which have sought new models based on physical concepts, as a way to avoid speaking about "negative losses". Herwing and Schmandt [1], showed that the origin of the negative sign was a diffusive shear work exchange between the two streams of a branched junction. Traditionally, the head losses at the branched junctions are neglected, but definitely it cannot be done in HVAC air-duct networks.

Firstly, the paper illustrates how, by ignoring this "negative loss" contradiction, traditional duct network analysis may encounter unexpected numerical difficulties. Secondly, it shows that the Minimum Energy Dissipation Principle (MinEDP) can be successfully applied to analyze the steady-state of any flow network (not necessarily HVAC ductworks), with or without shear work at junctions. Moreover, the new method does not need to know the latter, beforehand, although the nature of the solution is very different in either case.

Finally, the paper includes a practical example of an HVAC ductwork to illustrate the outcomes. The new method works smoothly and quickly and does not need any ad hoc modification to cope with an eventual "negative" head loss.

1. Introduction

1.1. Motivation, goals and the MinEDP

Within the EU project EE-Metal [3], seven partners belonging to the metal-mechanic sector (from France, Italy, Poland and Spain), collaborated between 2016–2019 in searching for energy efficiency measures stemmed from field-based audits. Document D2.6 of [3], HVAC section, concludes that ventilation sub-systems have a big improvement potential. Besides the energy saving target, the unprecedented covid-19 pandemic has also put the focus on the relationship between the ventilation systems and human health. Just to mention one of the many concerns; most of the "airborne infection isolation rooms (AIIR)" also known as "negative-pressure rooms" in hospitals were checked, and it was discovered that they were not so negative or even had a positive pressure. This flaw was already known many years before covid-19 (see [4]), but it was just overlooked. Dealing with the AIIR performance and the EE-Metal objectives, implies the correct *analysis* of flow HVAC duct networks.

Providing the engineering practitioners with good HVAC-ductwork analysis tools is, thus, crucial. During the development of the tools using standard techniques, some unexpected difficulties came across (see Appendix A). They were bypassed by an ad hoc patch, but it did not seem a neat solution.

- What is the origin of the troublesome eventualities?
- Is there any generalized method for dealing with them?

The short answer to the first question is the existence of a work interaction at the branched junctions. The head *loss* at the branched junctions is usually discarded but, in air duct systems, it cannot be done. This interaction sometimes shows up as a *negative* head *loss* coefficient. This eventual *negative* sign was the source of our difficulties. Despite a *negative* head *loss* looks indicative that

* Corresponding author.
E-mail address: vsoto@ter.upv.es (V.-M. Soto-Francés).

https://doi.org/10.1016/j.enbuild.2021.111504
0378-7788/

Nomenclature

Acronyms

$\bar{v}$	Average velocity $[m/s]$
Δp	Pressure drop $[Pa]$
$\dot{D}$	Diffusive shear work exchanged between the streams of the junction $[W]$
$\dot{S}_D$	Entropy production rate $[W/K]$
$\mathbb{F}$	Generalized local energy rate function per unit volume flow rate $[Pa]$
A	Cross-sectional area $[m^2]$
a,a'	Correction factors
C	Coefficient
d	Diffusive shear work exchanged between the streams of the junction per unit mass flow rate $[J/kg]$
d_{13}	Diffusive shear work received by a stream flowing from ① to ③ $[J/kg]$
e_m	Mechanical energy per unit mass $[J/kg]$
F	Generalized global energy dissipation rate per unit volume flow rate $[Pa]$
$f_{D,i}$	Darcy's friction factor at straight conduit at the i-section of the network
g	Linear map between the independent variables and the flow ratios at each network section
h	Function which maps each component of its argument to its absolute value
K	Energy dissipation factor per unit of mass $[J/kg]$
m_{fit}	The Afzal's universal relation for the Darcy's friction factor is fitted to the power law: $f_D = K_{fit} \cdot Re_\phi^{m_{fit}}$ (see the details in [2])
$nsect$	Amount of sections in the network

Greek Symbols

α	Non-dimensional correction factor for the kinetic energy
$\dot{\Phi}$	Energy dissipation rate $[W]$
ν	Kinematic viscosity $[kg \cdot s^{-1} \cdot m^{-1}]$
ψ_i	Volume flow rate ratio at section i, $\psi_i = \dot{V}_i/\dot{V}_T$
ρ	Density $[kg/m^3]$
φ	Energy dissipation per unit mass $[J/kg]$

Superscripts

†	External model for energy dissipation
$\dot{}$	The magnitude per unit time
$\hat{}$	The magnitude per unit volume

Subscripts

$\underline{ij}$	Magnitude referred to the flow rate flowing through ⓘ and ⓙ
φ	Pure dissipative
aux	Auxiliary
d	Shear work exchange
eq	Equivalent
sol	Solution
T	Total
t	Test point

something is not correctly managed, it has been overlooked for long because of its "hidden" nature (see subsection 2.1).

The response to the second question, is the use of the *Minimum Energy Dissipation Principle (MinEDP)*. The detailed explanation of the theory behind the MinEDP is out of the paper's scope. The interested reader may find many literature elsewhere. A chapter in book [5] summarizes the idea as: "The concept of minimum energy dissipation rate principle is that, when an open system is at a steady non-equilibrium state, the energy dissipation rate is at its minimum value. The minimum value depends on the constraints applied to the system. If the system deviates from the steady non-equilibrium state, it will adjust itself to reach a steady non-equilibrium state. The energy dissipation rate will reach a minimum value again." In other words, once one or more volume flow rates are fixed (see [6]) the flow distribution and pressure drops correspond to the minimum of the energy dissipation allowed by any constraints.

This paper is based on our previous works [2,6] for dissipating flow networks without shear work exchange and extends the outcomes to general networks with internal work exchange at their branched junctions.

1.2. The new paradigm which extends the steady state flow distribution analysis

The traditional method based on the energy balances (Bernoulli's equation), checks that the head loss between two points of a network is the same regardless of the path.

Unfortunately the current definition of the junction head *loss* coefficients, allows negative *losses* and, roughly, it may eventually lead to a negative hydraulic resistance inside a square root, thus crashing prematurely the search process for the solution. In short or simply stated: the classical concept of hydraulic resistance breaks down when branched junctions are included. Thus, any method which uses this concept has to cope with this internal flaw. However, our proposal based on the MinEDP leads to a unifying extremal principle which finds exactly the *same solution as before*, but in a very robust way.

Moreover, like other extremal principles in physics, it provides new insights about the problem. For instance, the work by Herwing and Schmandt [1] implicitly suggests that the correct modeling of the physical phenomena inside a branched junction needs three parameters (two dissipations and one work exchange) while for classical methods just two (the head *loss* at each branch) suffice to do the job. The MinEDP reconciles both views. Unfortunately, its proof is not straightforward and it will be done in another paper. Therefore, this paper is *not* about just a new or better way of doing the same old things. It additionally shows that the traditional solution is located at the minimum of the energy dissipation function, with the work exchanged at the branched junctions as an implicit internal constraint and proposes a solution method which deals smoothly with this constraint.

To our knowledge, this is the first *practical formulation* of an extremal principle which includes the effects of branched junctions.

In our opinion this paper could also be, along with [2] [6], a turning point about the way engineers deal and understand the flow distribution in networks.

1.3. Structure of the paper

Next Section 2 explains the details of the new method. Subsection 2.1 reviews the state of the art of modeling branched junctions. It shows how several authors have pointed out the need

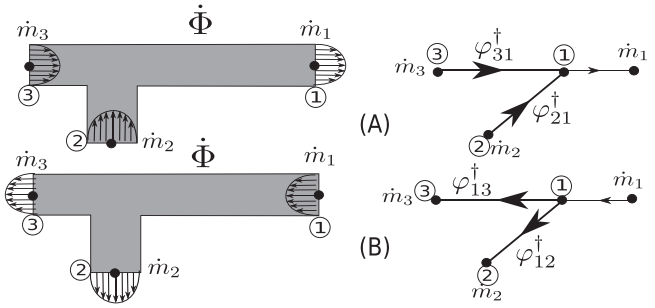

Fig. 1. External or conventional model. (A) Converging T-junction (B) Diverging T-junction. 1 common port, 3 main port, 2 branch port.

for a better model or understanding than just the head loss coefficient. Through a simple example, Appendix A shows how the negative sign of the coefficient, leads to computational difficulties. Based on this difficulties, subsection 2.2 compares a new branched junction model with the traditional one. The Bernoulli's equation is modified using this new model in subsection 2.3. The next two subsections 2.4 and 2.5 are key to prove that the MinEDP is equivalent, under certain conditions, to the modified Bernoulli's equation, developed previously in Section 2.3. Up to this point the proof is performed on an instance of a tree-shaped network for exposition simplicity. Subsection 2.6 generalizes the previous outcomes to any network type.

Section 3 briefly elaborates on the previous outcomes and some additional ideas.

Finally, Appendix B, illustrates the application of the MinEDP method through an example. Incidentally, Appendix B.1 clarifies the relationship among the traditional dissipation[1] $\widehat{\varphi}^{\dagger}$ (commonly known as pressure drop Δp), the head loss coefficient[2] $\widehat{C}$ and the energy factor $\widehat{K}^{\dagger}$.

To get a much more detailed idea about the whole MinEDP development, the reader is strongly referred to our previous works [2,6].

2. Methodology

2.1. Branched junctions: review and state of the art

The well-known methods for flow network analysis neglect the interaction effect at the branched junctions. However this is not always possible as in HVAC ductworks. Recently, Meulman's thesis [7] mentions that the interaction is important in many types of networks not only HVAC ductworks. Meulman also studies how to modify the conventional methods to incorporate the junctions.

Jaroslav Stigler [8] published an interesting and critical paper about the traditional model of the T-junctions. He argued:"They have not changed for more than 50 years. They have been derived on the base of unrealistic assumptions.". Assuming that all ports are at the same height (see Fig. 1): The energy losses, for the diverging case, are empirically evaluated based on the energy balance Eq. (1):

$$\dot{\Phi} = \rho \cdot \dot{V}_1 \left(\frac{\alpha_1 \bar{v}_1^2}{2} + \frac{p_1}{\rho} \right) - \rho \cdot \dot{V}_3 \left(\frac{\alpha_3 \bar{v}_3^2}{2} + \frac{p_3}{\rho} \right) - \rho \cdot \dot{V}_2 \left(\frac{\alpha_2 \bar{v}_2^2}{2} + \frac{p_2}{\rho} \right) \quad (1)$$

after discounting the losses due to the straight conduits (also known as friction losses), $\dot{\Phi}_{fitting}$ (also known as shape losses) is obtained and the *head loss coefficient* C_P of the fitting, is defined with respect to the common port ① as:

$$\dot{\Phi}_{fitting} = \rho \cdot \dot{V}_1 \cdot C_P \cdot \frac{\alpha_a \bar{v}_1^2}{2} = \dot{V}_1 \cdot \underbrace{\widehat{C}_P \cdot \frac{\alpha_a \bar{v}_1^2}{2}}_{\widehat{\varphi}^{\dagger}} = \widehat{\varphi}^{\dagger} \cdot \dot{V}_1 = \varphi^{\dagger} \cdot \dot{m}_1 \quad (2)$$

In practice a single value is not enough to characterize the junction, thus:

$$C_P = \frac{\dot{V}_3}{\dot{V}_1} C_{P_{31}} + \frac{\dot{V}_2}{\dot{V}_1} C_{P_{21}} = \psi \cdot C_{P_{31}} + (1 - \psi) \cdot C_{P_{21}} \quad (3)$$

where $C_{P_{31}}$ and $C_{P_{21}}$ are the traditional head loss coefficients in each branch referred to the common one ①. Stigler was conscious about the problems related with this split: "They (the head loss coefficients) could be less than zero therefore they cannot be treated as loss coefficients". This has caused historically discussions among researchers (see [9–11]). Stigler's alternative was to use external and physically meaningful magnitudes: C_P and the momentum coefficient C_M, which measures the force component exerted by the fluid over the junction in the direction of the common conduit. Unfortunately, although in [12] he shows how to estimate them, there is no clear practical application. In a recent review [13] of the Rennels and Hudson book, it is shown how C_P and C_M can be used along with semi-empirical correlations to obtain the traditional $C_{P_{31}}$ and $C_{P_{21}}$ (see chapter 16). In [14,15] experimental setups are described. Dordevic et al. [16] made an important effort to characterize the shape losses using exclusively the dissipation function. Unfortunately, for branched junctions, they forgot to include the key term shown in Eq. (4):

$$\dot{D} = \int_A \overline{\overline{\tau}} \cdot \vec{v} \cdot d\vec{A} \quad (4)$$

The meaning of $\dot{D}$ is the diffusive work transfer between the two branches as a consequence of the shear stress tensor $\overline{\overline{\tau}}$. This term may cause $C_{P_{31}}$ or $C_{P_{21}}$ to become negative. Gan and Riffat [17] tried to obtain both coefficients from CFD, but later on, Schmandt and Herwig [1] made something similar but, in our opinion, much more enlightening. Their model included Eq. (4), in a ingenious way: a tracer variable was used to distinguish both streams. In doing so, they could compute the diffusive work power $\dot{D}$ exchanged (or their work *interaction*, for short) and also assign different energy dissipation to each branch. They named the volumetric form of Eq. (4) $\dot{D}''' = \nabla \cdot \left(\overline{\overline{\tau}} \cdot \overline{v} \right)$, the local stress work rate and its specific value per unit of mass was called $d = \int \dot{D}''' \cdot dV/\dot{m}$. Moreover Herwig and Schmandt [18,19] proposed to relate, directly, the losses with the entropy production. The energy dissipation[3] and the entropy production are related by $\varphi = (T/\dot{m}) \cdot \dot{S}_D$. This relationship allows to identify where the dissipation is taking place (see [20]).

Herwig and Schmandt's ideas will be used in subsection 2.2 to define a model which fulfills the Stigler's target. Unfortunately, it might seem that a CFD calculation is needed to make the Herwig and Schmandt's split, thus pushing the solution of the problem back to the start. However, conceptually, it is a crucial step. In another paper, it will be proven that, in fact, no CFD is really needed. Anyhow, in practice, the traditional coefficients suffice and, in agreement with Herwig and Schmandt, they should be renamed as *head change coefficients*.

[1] for coherence, we keep the nomenclature close to [1,2] $\widehat{\varphi}^{\dagger}$ (see ahead).

[2] Idelchick head loss coefficient ζ correspondence $C = \widehat{\varphi}^{\dagger}/(\rho \bar{v}^2/2) = \zeta = \Delta p/(\rho \bar{v}^2/2)$.

[3] The difference between $\varphi^{\dagger}$ and φ will be explained ahead

2.2. The internal, external and dissipation model of a branched junction

This section contains, partially, knowledge which is not widespread in the field. It will be presented in a suitable way for a better understanding.

On one hand, the traditional head change (formerly *loss*) coefficients of many junction types, can be found in a very well-known handbook by Idelchik (note: many editions exist, [22]). This traditional model will be called *extern* because its parameters can be directly measured in the lab. For a two branched junction, it requires only two: the head change on each branch.

On the other, there exists a new proposal by Herwig and Schmandt [1] that will be called *internal*, which requires four parameters, instead of the previous two.

Finally, regardless of the model chosen, all the parameters can be referred to the flow rate at the common branch or to the flow rate at the corresponding branch.

Let's review the *internal* model. Comparing the traditional *external* model of Fig. 1 and the *internal* model shown in Fig. 2 the differences should be clear: the latter has an extra symbol $\dot{D}$ and the φ has no † superscript. As mentioned in subsection 2.1, $\dot{D}$ is the diffusive shear work exchanged between both streams and its value per unit of mass flow rate is written $d = \dot{D}/\dot{m}$. For the convergent junction ((*A*) in Fig. 2) the energy balance equation per unit of mass is written as[4] (see [1]):

$$\begin{aligned} e_{m,3} - e_{m,1} &= \frac{p_3}{\rho} - \frac{p_1}{\rho} + \frac{\alpha_3 \bar{v}_3^2}{2} - \frac{\alpha_1 \bar{v}_1^2}{2} + gz_3 - gz_1 = \varphi_{31} - d_{31} = \varphi^{\dagger}_{31} \\ e_{m,2} - e_{m,1} &= \frac{p_2}{\rho} - \frac{p_1}{\rho} + \frac{\alpha_2 \bar{v}_2^2}{2} - \frac{\alpha_1 \bar{v}_1^2}{2} + gz_2 - gz_1 = \varphi_{21} - d_{21} = \varphi^{\dagger}_{21} \end{aligned} \tag{5}$$

The Herwig and Schmandt's split allows to assign the dissipation and the work exchanged to each stream independently. The tracer variable used in their CFD generates a virtual boundary between both streams. By e_m we mean the energy per unit mass. Now the relationship between the formerly head *loss* $\varphi^{\dagger}$ and the actual energy dissipation φ can be clearly stated as:

$$\varphi^{\dagger} = \varphi - d \tag{6}$$

Therefore the conventional methods do not split the *pure* dissipation φ, which is an actual loss, from the diffusive work exchanged *d*. They just misinterpret $\varphi^{\dagger}$ as a loss. At first sight, it seems that a CFD computation is needed to make such split (as Herwig and Schmandt [1] did) but it is not. This paradox is quite hard to work out, but by using the MinEDP and the conventional head change (*loss*) coefficients, it can be proven that is actually possible to solve for *d*. However, the details fall out of the paper scope. Well, in fact, since $\dot{D}$ is an internal work exchange, d_{31} and d_{21} are not independent. Their relationship is:

$$\begin{aligned} &\dot{m}_3 \cdot d_{31} = -\dot{m}_2 \cdot d_{21} = \dot{D} = \dot{V}_3 \cdot \widehat{d}_{31} = -\dot{V}_2 \cdot \widehat{d}_{21} \\ &\widehat{d}_{31} \cdot \dot{V}_3 + \widehat{d}_{21} \cdot \dot{V}_2 = 0 \end{aligned} \tag{7}$$

So now, there seems that the *internal* model still has three independent parameters and thus, an extra degree of freedom remains. Otherwise stated, many internal combinations of the dissipation and work exchanged may lead to the same head change (*loss*) coefficients. However this is not so, because the MinEDP closes the problem.

Eq. (7) for a branched junction, given $\dot{m}_1 = \dot{m}_2 + \dot{m}_3$ and defining the flow rate ratio $\psi_2 = \dot{V}_2/\dot{V}_1 = \dot{m}_2/\dot{m}_1$ can be written per unit volume or mass as follows:

[4] $\alpha \approx 1$ for turbulent flows

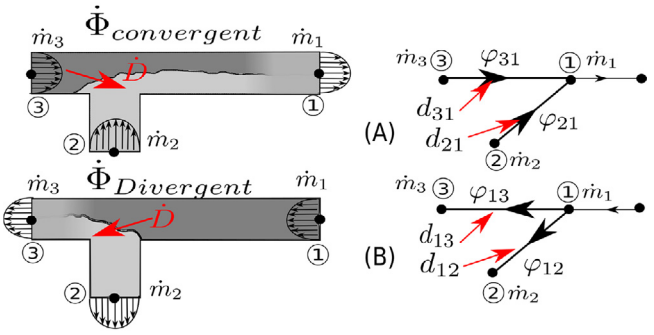

Fig. 2. Internal model: (A) Converging T-junction (B) Diverging T-junction. 1 common port, 3 main port, 2 branch port.

$$\begin{aligned} &\widehat{d}_{31} \cdot (1 - \psi_2) + \widehat{d}_{21} \cdot \psi_2 = 0 \\ &d_{31} \cdot (1 - \psi_2) + d_{21} \cdot \psi_2 = 0 \end{aligned} \tag{8}$$

Logically, since $0 \leqslant \psi \leqslant 1$, Eq. (8) means that if $\widehat{d}_{31} = d \cdot \rho > 0$ then $\widehat{d}_{21} < 0$ and vice versa. In words, one stream receives the work supplied by the other, thus its sign indicates the sense of the interaction. Finally, by definition, $\widehat{\varphi} = \varphi \cdot \rho > 0$, nevertheless $\widehat{\varphi}^{\dagger}$, at some branch, might be negative. This occurs if the work *d* is greater than the *pure* dissipation φ at that branch (see Eq. (6)). In this latter case, the head *change* coefficient *C* at that branch, becomes negative, although logically, the overall junction dissipates energy. In general, when there is a *d* transfer between the two streams, from an external standpoint, it seems that the stream which supplies the work, dissipates "more" (losses more energy) and the other less and one might get the misleading conclusion that $d = 0$.

In the same way, as the *C* coefficients were defined, two new types can be defined: the (pure) dissipation or (actual) head loss coefficient C_{φ} and the diffusive work coefficient C_d. What are the relationships between both types?.

The conventional or external model establishes for the head change at the *i*-branch $i \in \{2,3\}$, referred to the common branch ① C_{i1} the equation:

$$\begin{aligned} &C_{i1} = \frac{\varphi^{\dagger}_{i1}}{\bar{v}_1^2/2} = \frac{\varphi_{i1} - d_{i1}}{\bar{v}_1^2/2} = \frac{\varphi_{i1}}{\bar{v}_1^2/2} - \frac{d_{i1}}{\bar{v}_1^2/2} = C_{\varphi,i1} - C_{d,i1} \\ &\varphi_{i,1} = C_{\varphi,i1} \cdot \frac{\bar{v}_1^2}{2}, \quad d_{i1} = C_{d,i1} \cdot \frac{\bar{v}_1^2}{2} \end{aligned} \tag{9}$$

where $C_{\varphi,i1} > 0$ is the (pure) dissipation or loss coefficient and $C_{d,i1}$ is the work coefficient that can be null, positive or negative due to the sense of the interaction. Both are referred to the flow rate at the common branch. They can also be referred to the flow rate at its corresponding branch, symbolized by $C_{\underline{i1}}$.

$$C_{\underline{31}} = \frac{\varphi^{\dagger}_{31}}{\bar{v}_3^2/2} = C_{\varphi,\underline{31}} - C_{d,\underline{31}} = \frac{\varphi_{31} - d_{31}}{\bar{v}_3^2/2} = \frac{C_{31}}{(\bar{v}_3/\bar{v}_1)^2} \tag{10a}$$

$$C_{\underline{21}} = \frac{\varphi^{\dagger}_{21}}{\bar{v}_2^2/2} = C_{\varphi,\underline{21}} - C_{d,\underline{21}} = \frac{\varphi_{21} - d_{21}}{\bar{v}_2^2/2} = \frac{C_{21}}{(\bar{v}_2/\bar{v}_1)^2} \tag{10b}$$

Finally, for completeness, we include the relationship among the coefficients based on both reference systems (branch and common). Taking into account the continuity of the flow rates:

$$A_1 \cdot \bar{v}_1 = A_3 \cdot \bar{v}_3 + A_2 \cdot \bar{v}_2 \tag{11}$$

dividing by $\bar{v}_1$ and clearing for $\bar{v}_3/\bar{v}_1$ we get:

$$\frac{A_1}{A_3} - \frac{A_2 \cdot \bar{v}_2}{A_1 \cdot \bar{v}_1} \cdot \frac{A_1}{A_3} = \left(1 - \frac{\dot{V}_2}{\dot{V}_1}\right) \cdot \left(\frac{A_1}{A_3}\right) = \frac{\bar{v}_3}{\bar{v}_1} \tag{12}$$

therefore Eq. (10a) which expresses the relationship between both coefficients is:

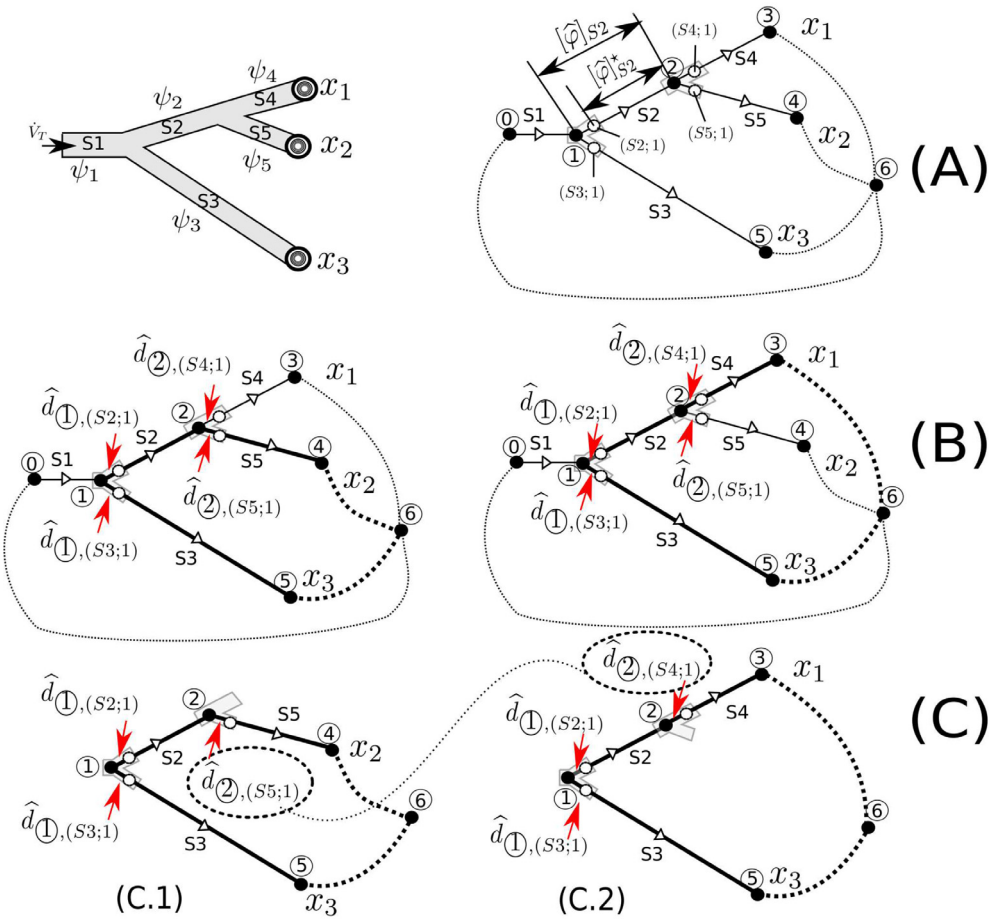

Fig. 3. Supply ductwork example to illustrate Bernoulli's principle for *intercating* branches: (A) Loops and flow senses $\psi_i = \dot{V}_i/\dot{V}_T, x$ supply flow rate ratio, (B) Interactions $\widehat{d}$, (C) Two independent loops $C.1$ and $C.2$, notice the work-link between the loops.

$$C_{\underline{31}} = C_{31} \cdot \frac{1}{\left(1 - \dot{V}_2/\dot{V}_1\right)^2 \cdot (A_1/A_3)^2} = C_{31} \cdot \frac{1}{(1-\psi_2)^2 \cdot (A_1/A_3)^2} \tag{13}$$

where $\psi_2 = \dot{V}_2/\dot{V}1$. Similarly for Eq. (10b) it can be written:

$$C_{\underline{21}} = C_{21} \cdot \frac{1}{\left(\left(\dot{V}_2 \cdot A_1\right)/\left(\dot{V}_1 \cdot A_2\right)\right)^2} = C_{21} \cdot \frac{1}{\psi_2^2 \cdot (A_1/A_2)^2} \tag{14}$$

Notice that the total junction dissipation is the same regardless of the type of coefficients (external or internal) and of the reference system (branch or common). Before going into the details of the MinEDP applied to interacting branches, next section employs this *internal* model, to solve the network steady-state, based on the traditional energy and mass balance.

2.3. Network steady-state: interacting branches (Bernoulli's principle)

The steady-state of a flow network is usually solved by Bernoulli's principle. Let's see how to write it anew but using the *internal* model. Instead of an abstract deduction, a simple supply ductwork, described in Fig. 3, will be used to illustrate the key idea. Some nodes are used as boundaries for each section of the network and are identified as ⓘ, while any j-node inside a k-section (Sk) is identified as (Sk;j). The energy losses (dissipation) along Sk are computed and labeled according to the following equation:

$$[\varphi]_{Sk} = \sum_{\text{All } j\text{-nodes within } Sk} \varphi_{(Sk;j)} \tag{15}$$

where $\varphi_{(Sj)}$ in Eq. (15), is the *pure* dissipation between nodes (Sk;j) and (Sk;$j-1$) within Sk (see Fig. 3(A)).

The total energy change in a loop or closed path must be zero. Without loss of generality, our example is a tree-shaped ductwork and ⑥ is a fixed-grade node, therefore on the right of Fig. 3 (A) the "pseudo-loops" are shown, which here, are just called loops. Looking at the bottom of Fig. 3, the following equations must hold for the ($C.1$)-loop:

$$\begin{aligned} e_{m,①} - e_{m,②} &= [\varphi]_{S2} - d_{①,(S2;1)} \\ +e_{m,②} - e_{m,⑥} &= [\varphi]_{S5} - d_{②,(S5;1)} \\ +e_{m,⑥} - e_{m,①} &= -[\varphi]_{S3} + d_{①,(S3;1)} \end{aligned}$$

$$0 = [\varphi]_{S2} + [\varphi]_{S5} - [\varphi]_{S3} - (d_{①,(S2;1)} + d_{②,(S5;1)} - d_{①,(S3;1)}) \tag{16}$$

where $d_{ⓙ,(Sk;1)}$ is the work received by the branch in section Sk between the node ⓙ and the first internal node, due to the other stream flowing through the other branch of the junction. The equation at the bottom of (16) is the sum of the three equations above it.

[4] $\alpha \approx 1$ for turbulent flows

Each left hand side represents the change in the specific mechanical energy $\Delta e_{m,ij} = e_{m,\textcircled{i}} - e_{m,\textcircled{j}}$, within a section between two nodes $\textcircled{i}\rightarrow\textcircled{j}$. The telescopic sum on the left side of Eq. (16) cancels out, since the sum is performed on a closed path. In a similar way, for the $(C.2)$-loop (bottom right of Fig. 3), the next equation holds:

$$0 = [\varphi]_{S2} + [\varphi]_{S4} - [\varphi]_{S3} - \left(d_{\textcircled{1},(S2;1)} + d_{\textcircled{2},(S4;1)} - d_{\textcircled{1},(S3;1)}\right) \tag{17}$$

Taking into account Eq. (6), dissipation and work terms can be joined in Eq. (17), and thus rewrite it as:

$$0 = [\varphi]^{\dagger}_{S2} + [\varphi]^{\dagger}_{S4} - \left([\varphi]^{\dagger}_{S3}\right) \tag{18}$$

Eq. (18) is a very well-known result, but its actual meaning is misunderstood. Written mistakenly without our † symbol seems to indicate a *loss*. Even, more plainly, multiplying by ρ and changing the symbol $\widehat{\varphi}^{\dagger}$ by the pressure drop: $0 = \Delta p_{S2} + \Delta p_{S4} - \Delta p_{S3}$. Engineers learn Eq. (18), in this latter form, by heart as: the energy dissipation or head loss along either path must be the same or, otherwise stated, the net head loss around any closed path must be zero. For instance, that would be the case for paths $\textcircled{1}-\textcircled{2}-\textcircled{3}-\textcircled{6}$ and $\textcircled{1}-\textcircled{5}-\textcircled{6}$ in loop $(C.2)$ of Fig. 3 (if the work interaction were not present). For the case of *non-interacting* branches, any d is zero and only then is correct to assume $\varphi^{\dagger} = \varphi$, i.e.,"*the dissipation is pure dissipation*". However, the interaction at the branched junctions actually exists, so that Eq. (18) cannot be interpreted naively, as just a head loss. Its equivalent *internal* Eq. (17) greatly clarifies things. The correct and overlooked interpretation is: the surplus net work received by the fluid in one path (for instance $\textcircled{1}-\textcircled{2}-\textcircled{3}-\textcircled{6}$) must equal the surplus energy loss along that path in order to balance the energy loss along both paths. It may also be restated as: the net head loss around any closed path must equal the net work received along that path. Moreover, strictly speaking, the traditional previous statement is just false for networks where the interaction is not neglected. Recall, incidentally, that $d_{\textcircled{1},(S2;1)} \neq d_{\textcircled{1},(S3;1)}$ (see Eq. (8)).

Finally, to solve the steady-state flow distribution of the example, there are only two independent loop flow rates, since the supply flow is fixed $\dot{V}_T$,. This relationship is made clear as: $x_1 + x_2 + x_3 = 1$, where $x = \dot{V}/\dot{V}_T$ is the supply flow rate ratio at each diffuser/grille. Therefore using the two Eqs. (16) and (17) for solving for two independent flow rates (for instance x_1 and x_2) is enough to solve the problem (see also our first paper [2] for the details). Notice that, by reversing the flow senses, a return network is obtained and the head change coefficients vary, but essentially the procedure to solve the problem is the same.

For completeness and better understanding, since it is not a widespread knowledge, next section gathers our main results [2], about the application of the MinEDP to *non-interacting* networks $(d = 0)$.

2.4. Network steady-state: non-interacting (MinEDP)-overview

The energy dissipation function of a flow network, where all its components are *pure* dissipative elements can be expressed as:

$$\dot{\Phi} = (\varphi_T \cdot \rho) \cdot |\dot{V}_T| = \sum_{j=1}^{nsect}\left([\varphi]_j \cdot \rho\right) \cdot |\dot{V}_j| = \sum_{j=1}^{nsect}[\widehat{\varphi}]_j \cdot |\dot{V}_j|$$
$$= \widehat{\varphi}_T \cdot |\dot{V}_T| > 0 \tag{19}$$

where the sum comprises all components of the network grouped by each of the *nsect* network sections. Taking the non-dimensional flow rate ratios ψ_j at each j-section, the previous equation can be rewritten as:

$$F(\psi_1, \psi_2, \ldots, \psi_{nsect}) = F\left(\vec{\psi}\right) = \frac{\dot{\Phi}}{|\dot{V}_T|} = \Delta p_T = \widehat{\varphi}_T$$
$$= \sum_{j=1}^{nsect}[\widehat{\varphi}]_j \cdot |\psi_j| > 0 \tag{20}$$

As before, $[\widehat{\varphi}]_j$ is the sum of the specific dissipations within the j-section. Recall that the ψ_j are not independent variables. Let us express the energy dissipation as a function of the $x_i, i \in \{1 \ldots n\}$ variables, since they are related directly with the desired flow rates at the diffusers. In non tree-shaped networks they can be the loop flows, see [6]. Notice that these are not yet independent variables, since some flow rates (not necessarily one), must be fixed beforehand. If, as in the previous example of subsection 2.3, the supply/return flow rate is fixed then just a single linear relationship exists $\sum x = 1$. Temporarily, in order to simplify the mathematics, let's assume that ψ_j does not change its sense (i.e. $\psi_j > 0$). Afterwards, in subsection 2.6, this constraint will be removed. So finally, Eq. (20), is written as:

$$(F \circ g)(x_1, x_2, \ldots, x_{n-1}) = F(g(\vec{x})) = \sum_{j=1}^{nsect}[\widehat{\varphi}]_j \cdot \psi_j(\vec{x}) > 0 \tag{21}$$

where there are $n-1$ independent variables. The original expression of F is now composed with a linear transformation $g : \vec{x} \rightarrow \vec{\psi}$. In paper [2] we showed that if the condition expressed by Eqs. (22) is fulfilled, then the dissipation function has a minimum and coincides with the steady-state flow distribution of the network. That is, the solution is the same as the one obtained by using the energy and mass balances.

$$\begin{aligned} \frac{\partial\widehat{\varphi}_j}{\partial\psi_j}\psi_j &= m \cdot \widehat{\varphi}_j \\ \frac{d\widehat{\varphi}_j}{\widehat{\varphi}_j} &= m \cdot \frac{d\psi_j}{\psi_j} \\ ln(\widehat{\varphi}_j) &= m \cdot ln(\psi_j) + ln\left(\widehat{K}_{\varphi,j}\right) = ln\left(\widehat{K}_{\varphi,j} \cdot \psi^m\right) \\ \widehat{\varphi}_j &= \widehat{K}_{\varphi,j} \cdot |\psi_j|^m > 0 \end{aligned} \tag{22}$$

In the deduction of Eq. (22) $\widehat{K}$, the energy dissipation factor, must be constant and positive. That is why we have emphasized this fact by using $\widehat{K}_{\varphi}$ instead of just $\widehat{K}$. The physical meaning of $\widehat{K}$ can be found in [2]. For a network of straight smooth conduits, [2] showed that specially defined values $\widehat{K} = \widehat{K}_{fit}$ and $m = m_{fit}$ can be fitted so that they remain constant for a huge Reynolds number range. In general, $\widehat{K}$ is not constant and the value of m actually does not matter (within some validity range) to solve the problem, (see [2]). Therefore by measuring or tuning the dissipation $\widehat{\varphi}$ with a law like Eq. (22), allows us to write Eq. (21) in the general and equivalent $\widehat{K}$-form:

$$F(g(\vec{x})) = \sum_{j=1}^{nsect}\left[\widehat{K}_{\varphi}\right]_j \cdot \psi_j^{m+1} > 0 \tag{23}$$

where $\left[\widehat{K}_{\varphi}\right]_j$ equals the sum of all $\widehat{K}_{\varphi}$ of the components in series inside the j-section. The fact that $\left[\widehat{K}_{\varphi}\right]_j$ is not constant, transforms the solution from a strict minimization into a sequence of minimizations, inside a global fixed-point problem. In concrete, given a certain test flow distribution $\vec{x}_t$, its associated *constant* vector is denoted as: $\overrightarrow{\widehat{\mathbb{K}}_{\varphi}}|_{\vec{x}_t} = \left(\left[\widehat{\mathbb{K}}_{\varphi}\right]_1, \ldots, \left[\widehat{\mathbb{K}}_{\varphi}\right]_{nsect}\right)|_{\vec{x}_t}$. Eq. 23 with $\overrightarrow{\widehat{\mathbb{K}}_{\varphi}}|_{\vec{x}_t}$ is labeled as $\mathbb{F}(\vec{x})|_{\vec{x}_t}$ and renamed as the "local" form of F. It is called

"local" because the physical phenomena which dissipate energy are "frozen" at the local point $\vec{x}_t$. The function $\mathbb{F}(\vec{x})|_{\vec{x}_t}$ has a minimum at $\vec{x}^*$. If this new flow distribution $\vec{x}^*$ is close to $\vec{x}_t$, or the other way round, the new $\vec{x}^*$ is coherent/compatible with the physics assumed by $\overrightarrow{\widehat{\mathbb{K}}_\varphi}|_{\vec{x}_t}$, then that is the steady-state solution. This can be seen as a fixed-point problem either in the flow distribution $\vec{x}$ or in the factor $\overrightarrow{\widehat{K}_\varphi}$.

2.5. Network steady-state: interacting branches (MinEDP)

This section extends the results of our previous paper [2], summarized previously in subsection 2.4.

Let's see first the expression for the energy dissipation function *F*. The dissipation function has the same form as Eq. 20 but in this case $[\widehat{\varphi}]_j$ should be the *pure* dissipation of the *internal* model. Now lets add the sum of the internal work exchanged at the branched junctions. This sum is, by definition, zero since it is an *internal* work exchange (see Eq. (8)) and thus we can write:

$$F(g(\vec{x})) = \overbrace{\sum_{j=1}^{nsect} [\widehat{\varphi}]_j \cdot \psi_j}^{\text{'pure' dissipation}} - \underbrace{\sum_{j=1}^{nsect} \widehat{d}_j \cdot \psi_j}_{\text{external work}=0} \tag{24}$$

Now, if in every *j*-section *Sj*, we separate from the sum $[\widehat{\varphi}]_j$, the term $\widehat{\varphi}_{\textcircled{k},(Sj;1)}$ corresponding to the dissipation at the *k*-branched junction and we rewrite the new sum as $[\widehat{\varphi}]_j^\star$, i.e., $[\widehat{\varphi}]_j^\star$, i.e., $[\widehat{\varphi}]_j = [\widehat{\varphi}]_j^\star + \widehat{\varphi}_{\textcircled{k},(Sj;1)}$ then:

$$\begin{aligned} F(g(\vec{x})) &= \sum_{j=1}^{nsect} [\widehat{\varphi}]_j \cdot \psi_j = \\ &= \sum_{j=1}^{nsect} [\widehat{\varphi}]_j^\star \cdot \psi_j + \sum_{j=1}^{nsect} (\widehat{\varphi}_{\textcircled{k},(Sj;1)} - \widehat{d}_j) \cdot \psi_j = \\ &= \sum_{j=1}^{nsect} [\widehat{\varphi}]_j^\star \cdot \psi_j + \sum_{j=1}^{nsect} \widehat{\varphi}^\dagger_{\textcircled{k},(Sj;1)} \cdot \psi_j = \\ &= \sum_{j=1}^{nsect} [\widehat{\varphi}^\dagger]_j^\star \cdot \psi_j + \sum_{j=1}^{nsect} \widehat{\varphi}^\dagger_{\textcircled{k},(Sj;1)} \cdot \psi_j = \\ &= \sum_{j=1}^{nsect} [\widehat{\varphi}^\dagger]_j \cdot \psi_j \end{aligned} \tag{25}$$

Notice that for any component, inside the *j*-section which does not belong to a branched junction, there is no work interaction and thus it is true that: $[\widehat{\varphi}]_j^\star = [\widehat{\varphi}^\dagger]_j^\star$. As expected, Eq. (25) means that the dissipation function can still be computed with the traditional coefficients. More clearly stated: *The energy dissipation function of the network is the same, regardless of the type of the coefficients employed; the head loss (internal) or the head change (external) coefficients.* Therefore, by direct extrapolation, similarly to the Eq. (23), Eq. (25) can also be written in *K*-form as:

$$F(g(\vec{x})) = \sum_{j=1}^{nsect} \left[\widehat{K}^\dagger\right]_j \cdot \psi_j^{m+1} > 0 \tag{26}$$

Like in the previous subsection 2.4, $\widehat{K}^\dagger$, in general, is not constant. Moreover, notice that although Eq. (23) looks like Eq. (26), the latter has a work interaction subtly included inside the $\widehat{K}^\dagger$. The difference in the notation of the $\widehat{K}$ terms in both equations, makes explicit that they have a different physical meaning. Nevertheless, in numerical form, both are easily confused, since both are used to compute the energy dissipation.

Obviously, some questions show up: under what conditions the minimization of Eq. (26) or (25) is equivalent to the results in subsection (2.3)?. Has got, adding the total *internal* work, any effect on the results?.

Instead of using a completely general mathematical formulation, let's use the same example of subsection 2.3. Taking Eq. (24), the conditions for the stationarity of the dissipation function for that example are: $\partial F/\partial x_1 = 0$ and $\partial F/\partial x_2 = 0$. In order to simplify the notation instead of $\widehat{d}_{\textcircled{k},(S_j;1)}$ let's just write $\widehat{d}_j$ for the work interaction at the branch in the *j*-section. Thus, writing only the partial derivative with respect to x_1:

$$\begin{aligned} \frac{\partial F}{\partial x_1} &= \left(\frac{\partial [\widehat{\varphi}]_2}{\partial \psi_2}\psi_2 - \frac{\partial \widehat{d}_2}{\partial \psi_2}\psi_2 + \frac{\partial [\widehat{\varphi}]_4}{\partial \psi_4}\psi_4 - \frac{\partial \widehat{d}_4}{\partial \psi_4}\psi_4 - \frac{\partial [\widehat{\varphi}]_3}{\partial \psi_3}\psi_3 + \frac{\partial \widehat{d}_3}{\partial \psi_3}\psi_3 \right) \\ &\quad + \left([\widehat{\varphi}]_2 + [\widehat{\varphi}]_4 - [\widehat{\varphi}]_3 - \left(\widehat{d}_2 + \widehat{d}_4 - \widehat{d}_3\right) \right) \\ &= 0 \end{aligned} \tag{27}$$

Now, let's keep the same assumption as in subsection 2.4 for the *pure* dissipation term, that is: it fulfills the same expression (22). Similarly, some assumption must be taken for the diffusive shear work $\widehat{d}_j$ and there is no loss of generality by considering that it follows a similar law. In fact, such assumption is necessary, as it will be shown below, to group both $\widehat{\varphi}$ and $\widehat{d}$ into the conventional $\widehat{\varphi}^\dagger$. In the following derivation, the sign of $\widehat{d}_j$ indicates the sense of the work and therefore it can be chosen as positive (i.e. received by the branch):

$$\begin{aligned} \widehat{\frac{\partial d_j}{\partial \psi_j}}\psi_j &= m \cdot \widehat{d}_j \\ \widehat{d}_j &= \widehat{K}_{dj} \cdot |\psi_j|^m \end{aligned} \tag{28}$$

Notice, nevertheless, that $\widehat{K}_{dj}$ may be positive or negative, depending on the sense of the work interaction, but $\widehat{K}_{\varphi j}$ is always positive. According to our hypotheses, both $\widehat{K}_{dj}$ and $\widehat{K}_{\varphi j}$ must be constant in Eq. (28) and (22), respectively. Finally, if both hypotheses are fulfilled then Eq. (26) is transformed into $\mathbb{F}|_{\vec{x}_t}$ the "local" version of the dissipation function *F*. As before, the suffix $\vec{x}_t$ indicates that $\mathbb{F}$ depends on the flow distribution point where $\widehat{K}_\varphi$ and $\widehat{K}_d$ are evaluated, or in order words, by keeping these factors constant, the physical dissipation and work transfer mechanisms are "frozen" at their local values at $\vec{x}_t$. The function $\mathbb{F}|_{\vec{x}_t}$ represents the "local" behavior of the system.

The $\mathbb{F}$ stationary condition (for the same example of subsection 2.4), converts Eq. (27) into:

$$\frac{\partial \mathbb{F}}{\partial x_1} = (m+1) \cdot \left([\widehat{\varphi}]_2 + [\widehat{\varphi}]_4 - [\widehat{\varphi}]_3 - \left(\widehat{d}_2 + \widehat{d}_4 - \widehat{d}_3\right) \right) = 0 \tag{29}$$

If the terms $\widehat{\varphi}_j$ and $\widehat{d}_j$ for the branched element of the *j*-section are grouped, we get the important relationship for $\widehat{K}_j^\dagger$ at the *j*-branch of the junction:

$$\widehat{\varphi}_j^\dagger = \widehat{\varphi}_j - \widehat{d}_j = \widehat{K}_{\varphi j}|\psi_j|^m - \widehat{K}_{dj}|\psi_j|^m = \widehat{K}_j^\dagger \cdot |\psi_j|^m \tag{30}$$

This latter equation means that, whenever the conventional head *change* coefficient is used, i.e. by computing $\widehat{K}_j^\dagger$, then it is also assumed implicitly that the work exchange, at the junction, follows a potential law. We would like to stress that although Eq. (30) looks like Eq. (22), *they are not equal*. Even when the energy factor $\widehat{K}$ is positive in both cases, their physical meaning is completely different and a source of confusion. In Eq. (22) $\widehat{K}$ is an energy *dissipation* factor, while in Eq. (30), it is *just an energy factor*.

Taking into account that for the rest of the elements in series within a section $\widehat{\varphi} = \widehat{\varphi}^{\dagger}$, i.e. there exist only *pure* dissipation, Eq. (29) is written as:

$$\frac{\partial \mathbb{F}}{\partial x_1} = (m+1)\cdot\left(\left[\widehat{\varphi}\right]_2^{\dagger} + \left[\widehat{\varphi}\right]_4^{\dagger} - \left[\widehat{\varphi}\right]_3^{\dagger}\right) = 0 \tag{31}$$

Notice that Eqs. (29) and (31) are equal to the Eqs. (17) and (18) respectively. An analogous result would be obtained for the other partial derivative $\partial\mathbb{F}/\partial x_2 = 0$. Therefore, by generalizing, we get a very important result: *each partial derivative of* $\mathbb{F}$ *corresponds to one energy balance at an independent loop of the network. Minimizing a "local" form of Eq. (25), using the traditional head change coefficients (which lead to* $\widehat{K}_j^{\dagger}$*, see Section Appendix B.1) is equivalent to the energy balance at each independent loop, including any work exchange.*

Solving the problem can be accomplished as in section subsection 2.4, by a sequence of minimizations steps, inside a global fixed-value problem. In other words, an initial point $\vec{x}_0$ is assumed and $\mathbb{F}|_{\vec{x}_0}$ is computed. If the solution $\vec{x}^*$ to the minimization step of $\mathbb{F}|_{\vec{x}_{n-1}}$ is not compatible or coherent with the constant vector $\overrightarrow{\widehat{\mathbb{K}}^{\dagger}}$ computed at $\vec{x}_{n-1}$, a new $\overrightarrow{\widehat{\mathbb{K}}^{\dagger *}}$ is computed at $\vec{x}^* = \vec{x}_n$ and a new minimization step is performed until $\vec{x}^* \approx \vec{x}_{n-1}$ or $\overrightarrow{\widehat{\mathbb{K}}^{\dagger}} \approx \overrightarrow{\widehat{\mathbb{K}}^{\dagger *}}$.

At first sight, it may seem that the steady-state solution of the network is going to be a minimum of the dissipation function *F*, but unlike the non-interacting case, is not. Let's see more in detail what is going on. Recall that the solution is a sequence of minimization problems of an approximate or "local" dissipation function $\mathbb{F}$. This function is formally like Eq. (26) but any $\widehat{K}_j^{\dagger}$ is kept constant $\widehat{\mathbb{K}}_j^{\dagger}$. Thus, the $\mathbb{F}$ has the form:

$$\begin{aligned}\mathbb{F}(g(\vec{x})) &= \sum_{j=1}^{nsect}\left[\widehat{\mathbb{K}}\right]_j^{\dagger}\cdot\psi_j^{m+1} \\ &= \overbrace{\sum_{j=1}^{nsect}\left[\widehat{\mathbb{K}}\right]_{\varphi,j}\cdot\psi_j^{m+1}}^{=\text{dissipation}} - \underbrace{\sum_{j=1}^{nsect}\widehat{\mathbb{K}}_{d,j}\cdot\psi_j^{m+1}}_{=\text{external work}}\end{aligned} \tag{32}$$

Notice that this function is *not* the dissipated energy. The *external work* is not zero as in (24). The second sum in Eq. (32) is only zero at the flow distribution test point $\vec{x}_t$ where the vector $\mathbb{K}^{\dagger}$ was computed. During the minimization step the work factors $\widehat{\mathbb{K}}_d$ are kept constant and therefore you may think of the work received by the network as "external" and proportional to a power of the flow rate in the branch. Therefore conceptually minimizing Eq. (32) is equal to minimizing the dissipation and maximizing the "external work" received by the network, assuming as constant the physical mechanism by which the branches are currently dissipating energy and exchanging work. Therefore, after a minimization step, the "external" work is non-zero. Nevertheless, step by step the amount is reduced until the solution is reached. Obviously, at the solution there is no net "external" work applied to the branches. In other words, the solution must be on a hypersurface of the space represented by $\vec{x}\times F(\vec{x})$, or the global energy dissipation hyper-surface. Recall that, on this surface, the *net external work* is always zero (see the second sum in Eq. (24)).

It can be said that the proposed solution procedure is equivalent to a constrained minimization problem related with this *internal* work exchange. Therefore the network does not approach its minimum dissipation, since the internal work exchanged creates a bias in its tendency to minimize the energy dissipation. Let's make this point clearer. If Eq. (32) is rewritten as:

$$\nabla\mathbb{F} = \nabla(\text{dissipation}) - \nabla(\text{external work}) = 0 \tag{33}$$

then, the idea shows up. This equation after some iterations on $\vec{x}$ is also valid at the steady-state solution $\vec{x}_{sol}$. At this point is true that:

$$\nabla\mathbb{F}|_{\vec{x}_{sol}}(\vec{x}_{sol}) = \nabla(\text{dissipation})(\vec{x}_{sol}) - \nabla(\text{external work})(\vec{x}_{sol}) = 0 \tag{34}$$

$$\mathbb{F}|_{\vec{x}_{sol}}(\vec{x}_{sol}) = F(\vec{x}_{sol}) \quad ,\text{implicitly external work} = 0 \tag{35}$$

and therefore $\nabla(\text{dissipation})(\vec{x}_{sol}) = \nabla(\text{external work})(\vec{x}_{sol}) \neq 0$. This means that the dissipation is not a minimum at the steady-state, for a network with interacting branches. The physical meaning could be: *the work interaction at the branched junctions transfers energy from some branches to another ones so that globally the network dissipates more energy than without such interactions and in doing so, the net is able to re-balance itself.* Additionally, if the "local" approximation at the solution $\vec{x}_{sol}$, i.e. Eq. (35), is multiplied (scalar product) by vector $\Delta\vec{x}$, we get:

$$\begin{aligned}\nabla\mathbb{F}(\vec{x}_{sol})\cdot\Delta\vec{x} = \nabla(\text{dissipation})(\vec{x}_{sol})\cdot\Delta\vec{x} - \nabla(\text{externalwork}) \\ \times(\vec{x}_{sol})\cdot\Delta\vec{x} \\ = 0\end{aligned} \tag{36}$$

Eq. (36) could provide some extra insight about the nature of the steady-state. If the flow distribution makes a very small, "virtual", *displacement* in direction $\Delta\vec{x}$, assuming that the physical mechanisms present within the network for energy dissipation and work transfer remain the same, then the increase in the "external" work received by the network is balanced by an equal increase its energy dissipation, thus inhibiting such *displacement*. At the steady-state solution this is true for such "virtual" displacement in *any* direction and is coherent with a null "external" work.

Next section generalizes the previous result to any type of network, not simply tree-shaped ones.

2.6. Generalization for any network (not necessarily tree-shaped)

Without loss of generality, previously, it was assumed that ψ does not change its sign (reverses its sense), to simplify the exposition. This section relaxes that hypothesis. Eq. (21) is valid in general. To clarify what is the effect of using the absolute value of the flow rate ratios $|\psi_j|$, the function composition in (21) becomes:

$$(F\circ h\circ g)(x_1,x_2,\ldots,x_{n-1}) = F(h(g(\vec{x}))) = \sum_{j=1}^{nsect}\left[\widehat{\varphi}\right]_j\cdot|\psi_j| > 0 \tag{37}$$

which uses a new map $h:\vec{\psi}\to(|\psi_1|,\ldots,|\psi_{nsect}|)$. The derivative of *F* respect to $\vec{x}$ using the chain rule, and forcing the stationarity of *F* gives:

$$\mathscr{D}(F\circ h\circ g) = (\mathscr{D}F\circ(h\circ g))\cdot(\mathscr{D}h\circ g)\cdot\mathscr{D}g = \vec{0} \tag{38}$$

where $\mathscr{D}h$ is a diagonal matrix with an entry in each *j*-row equal to $\text{sign}(\psi_j)$. Now if the previous equation is applied to the example of subsection 2.4, its Eq. (27) is rewritten as:

$$\begin{aligned}\frac{\partial F}{\partial x_1} = &\begin{pmatrix} \frac{\partial\left[\widehat{\varphi}\right]_2}{\partial|\psi_2|}|\psi_2|\text{sign}(\psi_2) - \frac{\partial\widehat{d}_2}{\partial|\psi_2|}|\psi_2|\text{sign}(\psi_2) \\ +\frac{\partial\left[\widehat{\varphi}\right]_4}{\partial|\psi_4|}|\psi_4|\text{sign}(\psi_4) - \frac{\partial\widehat{d}_4}{\partial|\psi_4|}|\psi_4|\text{sign}(\psi_4) \\ -\frac{\partial\left[\widehat{\varphi}\right]_3}{\partial|\psi_3|}|\psi_3|\text{sign}(\psi_3) + \frac{\partial\widehat{d}_3}{\partial|\psi_3|}\psi_3\text{sign}(\psi_3)\end{pmatrix} \\ &+\left(\left[\widehat{\varphi}\right]_2\text{sign}(\psi_2) + \left[\widehat{\varphi}\right]_4\text{sign}(\psi_4) - \left[\widehat{\varphi}\right]_3\text{sign}(\psi_3)\right) \\ &-\begin{pmatrix}\widehat{d}_2\text{sign}(\psi_2) \\ +\widehat{d}_4\text{sign}(\psi_4) \\ -\widehat{d}_3\text{sign}(\psi_3)\end{pmatrix} = 0\end{aligned} \tag{39}$$

When the hypotheses which lead to the power laws for the energy dissipation and work exchanged, are applied to Eq. (39) we obtain the derivative of its "local" form $\mathbb{F}$:

$$\frac{\partial \mathbb{F}}{\partial x_1} = (m+1)\cdot \begin{pmatrix} [\widehat{\varphi}]_2 \text{sign}(\psi_2) + [\widehat{\varphi}]_4 \text{sign}(\psi_4) - [\widehat{\varphi}]_3 \text{sign}(\psi_3) \\ -\left(\widehat{d}_2 \text{sign}(\psi_2) + \widehat{d}_4 \text{sign}(\psi_4) - \widehat{d}_3 \text{sign}(\psi_3)\right) \end{pmatrix} = 0 \tag{40}$$

whose corresponding previous equation was (29). Finally Eq. (40) can also be written as:

$$\frac{\partial \mathbb{F}}{\partial x_1} = (m+1)\cdot \left(\text{sign}(\psi_2)[\widehat{\varphi}]_2^{\dagger} + \text{sign}(\psi_4)[\widehat{\varphi}]_4^{\dagger} - \text{sign}(\psi_3)[\widehat{\varphi}]_3^{\dagger}\right) = 0 \tag{41}$$

The important conclusion here is that Eqs. (40) and (41) are equal to the energy balances (17) and (18) respectively, but corrected with the $\text{sign}(\psi_j)$, so that in case of flow reversal, the energy balance is performed correctly. Therefore, the completely general expression of the dissipation is (37) and the minimization of its "local" form $(\mathbb{F}\circ h\circ g)(x_1, x_2, \ldots, x_{n-1})$ is equivalent to the correct energy balance, regardless of the final sense of the flow rate at each network section.

At first sight, the MinEDP method might look a bit complex but, in fact, is quite simple, robust and unifying. Although, the goal of the present paper is not going into the very details of a concrete calculation, Appendix B.2 is devoted to illustrate the ideas through an example.

3. Discussion

The paradoxical possibility of getting a *negative* head loss coefficient at branched junctions, has been controversial for long time [8–11]. In practice, it is frequently overlooked but is, also, a symptom that something is not being managed properly. Moreover, while developing an analysis assistant tool, numerical problems were encountered in HVAC duct networks, which stemmed from this possibility and the ignorance about the final flow distribution. Herwig and Schmandt [1], clearly identified the cause of the negative sign of the head loss coefficient as the diffusive shear work exchange. We wondered if there was a higher level principle which avoided such inconveniences, thus centering our research on a MinEDP formulation. Our approach was to increase the complexity gradually: first dealing with networks without interaction at the branched junctions, (see [2,6]) and then including them.

Notice that even when the traditional head loss coefficients are positive simultaneously at both branches, there may still exist a work exchange inside the junction. We acknowledge that this creates a lot of confusion and has contributed to overlook the issue. The paper defines two types of models: the conventional, called *external*, and the new called *internal*. The names point to the fact of being or not directly measurable, respectively. The conventional model just needs two independent parameters (the head loss/change coefficients at each branch) while the second "apparently" needs three, two (real) head *loss* coefficients and the exchanged work. This creates an apparent contradiction or paradox: how can the solution be found traditionally just with two parameters but now there is a need for a third?. The cost of the contradiction is allowing negative hydraulic resistances. Nevertheless, it can be solved by using the MinEDP method exposed here, but this will be proven in another paper, because it needs quite effort. Incidentally, as shown in the example, the conventional head loss coefficients are enough for our MinEDP methodology, so all flow resistance databases are still useful. However the *internal* model is needed to understand what is going on behind "the curtain". Based on the new *internal* model the traditional Bernoulli's analysis of flow networks can be rewritten. The minimization of the local form of the dissipation function, is proven to be equivalent to this new Bernoulli's set of equations. Additionally, the physical meaning attached to K indicates the existence of a fixed-point which represents the solution. In other words, the solution can be computed by performing a sequence of minimizing steps (equivalent to energy balances) of its "local" form $\mathbb{F}$ within a global fixed-point iteration (equivalent to matching the physical dissipation and work exchange mechanisms with those associated to the computed K).

After our paper [2], for non-interacting branches, the flow distribution solution coincides with the minimum of the "global" dissipation function F. In this case, the energy factors $\widehat{K}^{\dagger}$ are equal to the energy *loss* factors $\widehat{K}_{\varphi}$.

However, here it has been proven that if the branched junctions are included then the flow distribution does not coincide with the minimum of F. The problem becomes a constrained minimization one. The interesting fact, is that the procedure to solve the problem is exactly the same: a sequence of minimizing steps of the "local" form $\mathbb{F}$ of the "global" dissipation function F. Though, now, the energy factors $\widehat{K}^{\dagger}$ change their physical meaning, and this is *crucial*.

Notice that exponent m of the power-law employed to express the dissipation function (see Eq. (26)) does not really affect the result since it also modifies the K factors (the dissipation value does not depend on the chosen exponent). The role of m was shown in detail in our previous work [2]. It is the energy dissipation, along with the constraints, what determines the global solution. The exponent acts as a tuning parameter for the metric associated to the energy dissipation but does affect the convergence to the solution. In other words, in the general case m cannot be settled to fit simultaneously all the energy dissipation mechanism of the network and this creates the need for a fixed-point iteration.

Although the computational performance was not the goal of the paper, implementation in Scilab indicates very promising results. The calculation was very quick, simple to code and robust, since the solution was not sensible to the initial flow distribution point (see Appendix A).

Finally, the shear work exchange has "hidden" effects on the flow distribution, which some authors try to minimize [23], but could be foreseen with the new methodology.

4. Conclusions

- The paper shows that the steady-state of *any* flow network can be obtained with a practical method based on an extremal principle, the MinEDP. The solution is *exactly the same* as the one obtained by using the Bernoulli's equation. It avoids running into difficulties due to eventual negative hydraulic resistances during the search for the solution. It is a very robust method since the solution process does not depend on the assumed initial flow distribution.
- Moreover, the MinEDP formulation extends our knowledge about the nature of the flow distribution. When there is no work exchange at the branched junctions the steady-state is located at a minimum of the global dissipation function F, however this is not so when there exist work interactions. In other words, the system tries to minimize its dissipation rate but limited by the constraints imposed by those interactions.
- Based on the work of Herwing et al. [1], the paper formalizes the *internal* model for the branched junctions as a physically meaningful alternative to the head loss coefficients. Nevertheless, our method can still use the traditional head loss (change) coefficients.

  Although not proven here, it is worthwhile mentioning (because it seems a bit paradoxical) that the internal model can be obtained, if needed, by using the MinEDP as the closing equation. In other words, the work interaction is encoded inside the conventional coefficients and the MinEDP.

- The new methodology does not need to be aware of the work exchange at the junctions (the constraints). It can use the conventional head loss (change) coefficients found in many databases. The solution method is always the same (see [2]) and moves on to the constrained problem, naturally.

Declaration of Competing Interest

The authors declare that they have no known competing financial interests or personal relationships that could have appeared to influence the work reported in this paper.

Appendix A. The negative hydraulic resistances issue

This appendix illustrates the difficulties which arise from a negative hydraulic resistance, since they sparked this research.

A.1. Operating point of a fan duct-network

As mentioned in Section 1 difficulties arise due to some head change (*loss*) coefficient becoming negative (see [1]). Let's see the detailed explanation.

The concept of operating point as the intersection of the resistance curve of a flow network and the fan curve is widely spread in the literature (see Fig. A.4). A traditional way of obtaining this point can be summarized in five steps:

1. Guess a flow distribution and compute the hydraulic resistances.
2. (Compression step) Compute the duct-network characteristic curve.
3. Intersect the previous curve with the characteristic curve of the fan.
4. (Decompression step) Re-compute the flow rate at each section and at the terminals (diffusers and/or return grilles).
5. Return to step 1 until the initial guess and the new flow rates are nearly the same.

Let's assume that any j-element of the net fulfills the potential law shown in Eq. (A.1):

$$\Delta p_j = \widehat{K}_j \cdot \frac{\dot{V}_j^2}{A_j^2} \tag{A.1}$$

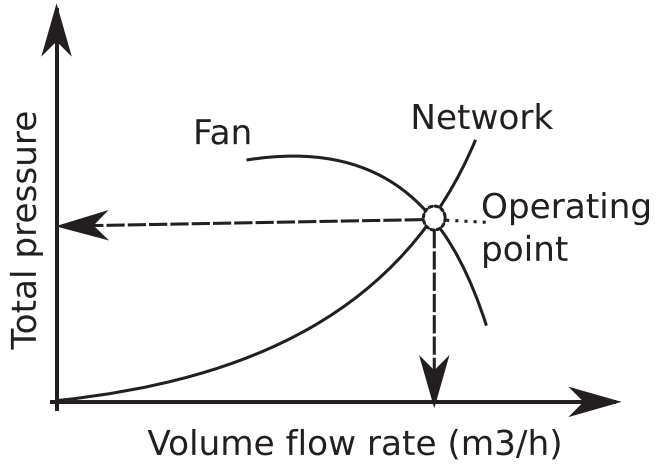

Fig. A.4. Operating point of a fan-duct network system.

Here by $\widehat{K}_j$ it is meant the loss at any; diffuser, fitting or straight conduit. In the case of a branched junction, the loss is split into the different branches. The equivalent resistance curve of the net has the same form as Eq. (A.1) and the flow $\dot{V}_T$ is the total flow of the supply or return network. This equivalent curve is obtained in step 2 (compression) using the equivalence between sections connected in series or in Y (parallel) (see Fig. A.5). The transformation equations are the following:

$$\widehat{K}_{eq} = \widehat{K}_i + \widehat{K}_j \cdot \left(\frac{A_i}{A_j}\right)^2 \tag{A.2}$$

for series, while for parallel (Y) the formula is:

$$\widehat{K}_{eq} = \widehat{K}_c + H_{i,j}^2 \cdot \widehat{K}_j \cdot \left(\frac{A_c}{A_j}\right)^2 \tag{A.3}$$

where:

$$H_{i,j} = \left[1 + \frac{A_i}{A_j} \cdot \sqrt{\left(\frac{\widehat{K}_j}{\widehat{K}_i}\right)}\right]^{-1} \tag{A.4}$$

The procedure is iterative since some $\widehat{K}_j$ may depend on the volume flow rate or/and the flow distribution (like in branched junctions). Notice that the same equations are used in step 4 to decompress the net. During this latter step, the flow through each branch is obtained as: $\dot{V}_i = H_{i,j} \cdot \dot{V}_c$ and $\dot{V}_j = \dot{V}_c - \dot{V}_i$. Everything works whenever Eq. (A.4) can be applied, i.e., the term inside the square root is positive.

In the next two sections, let us apply this procedure to a simple network.

A.2. Example (sizing-step)

Let us size the duct network shown at the top of Fig. A.6. The sizing is performed using the equal friction method with $\Delta p_{loss}/L = 1[Pa/m]$. The solution is drawn at the bottom of Fig. A.6. Table A.1 shows the parameters that characterize the elements of the ductwork. Table A.2 illustrates that at the lateral return paths, $X3$ and $X5$, the pressure loss due to the short straight ducts is not enough to compensate for the head increase at the junction (notice the negative values).

Obviously, the net needs to be balanced or, in other words, forced to get the desired design flows through each grille. The following dampers are needed; along the path $X1 - X3$ a loss of 21.15 $[Pa]$ is needed and can be obtained with a cross sectional area reduction ratio of 0.56, while in the path $X1 - X2 - X5$ the additional loss 12 $[Pa]$ needed can be obtained with a reduction ratio of 0.62. Therefore the design operating point would be after balancing: $\dot{V} = 1600\ [m^3/h], \Delta p_T = \Delta p_{supply} + \Delta p_{return} = 36.72 + 23.74 = 60.46\ [Pa]$.

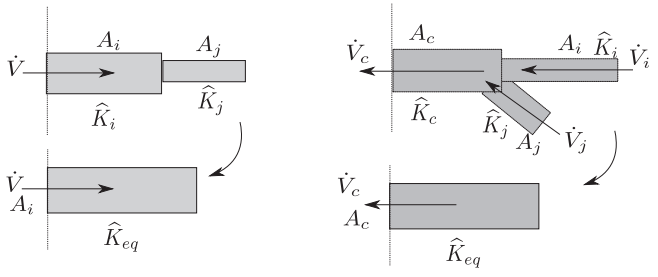

Fig. A.5. Equivalence transformation: Left) series, Right) Parallel.

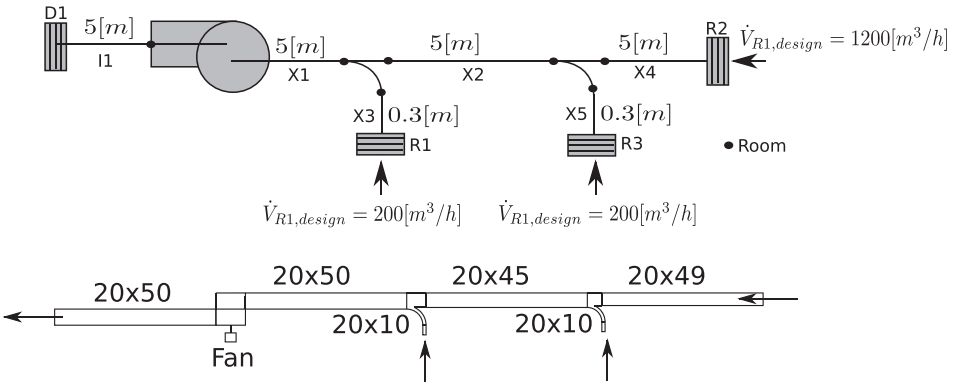

Fig. A.6. Example return network. Top: Geometrical layout and design flow rates. Bottom: top-view of the sized network.

Table A.1
Properties of the diffuser and return grilles of the example network.

Fitting	Name	Ref. $[m^3/h]$	Value at Ref. $[Pa]$
Diffuser	I1	1600	$\Delta p_{total} = 31.82$
Return grille	R1	200	$\Delta p_{static} = 1.73$
Return grille	R2	1200	$\Delta p_{static} = 2.05$
Return grille	R3	200	$\Delta p_{static} = 1.76$

At this point, practical questions usually arise: are these dampers really needed?, otherwise stated, after the sizing step: would the flow rates be close enough to the design ones without the dampers?. Therefore to answer these questions, the designer now needs to evaluate or analyze an already sized network.

A.3. Example (analysis-step): Difficulties

Before choosing a fan, we have to remove the dampers and force that the operating point is always at $\dot{V} = 1600\ [m^3/h]$. Now, the problem is to find out the actual flow distribution, i.e., an operating point. A bad initial guess, of the flow distribution, may lead during the Section Appendix A.1 iteration to $\widehat{K}_j < 0$ at some compression/decompression step. Eq. (A.4) could not be evaluated and therefore the computation crashes. This does happen with the previous network, if the design flow rates are used as the initial guess. Notice that this does not mean that there is no solution. It does have one, but the algorithm needs to be specially careful to surpass this eventual difficulty. Basically it needs a method to estimate a better guess when this exception occurs. Table A.3 shows the solution after this ad hoc solution is devised. Looking at the table it can be seen that there is a big difference between the design and the actual flows.

Last but not least, any procedure based on the operating point calculation as shown in Sections Appendix A.1 might find difficulties when dealing with branched junctions. Even before trying to analyze the net. For instance, some sizing methods use the operating point for sizing (designing) the ductwork. The T-method is an example. It uses a compression-optimization-decompression sequence, while trying to optimize the network size. However it has problems [21], including the one explained above.

Appendix B. Example

This appendix illustrates the ideas exposed in the paper through an example. The paper along with our previous works [2,6], are enough for the implementation of the method.

B.1. Relationships: $\widehat{\varphi}^{\dagger}, \widehat{C}, \widehat{K}^{\dagger}$

Using the head change coefficient of a converging fitting, referred to the branch ③-① $C_{\underline{31}}$ we have:

$$\begin{aligned} \widehat{\varphi}^{\dagger}_{\underline{31}} &= C_{\underline{31}} \cdot \rho \cdot \tfrac{\bar{v}_3^2}{2} = \widehat{C}_{\underline{31}} \cdot \tfrac{1}{2} \cdot \left(\tfrac{\dot{V}_3}{A_3}\right)^2 = \widehat{C}_{\underline{31}} \cdot \tfrac{1}{2} \cdot \left(\tfrac{\dot{V}_3}{\pi \cdot D_3^2/4}\right)^2 \cdot \left(\tfrac{\dot{V}_T}{\dot{V}_T}\right)^2 \\ \widehat{\varphi}^{\dagger}_{\underline{31}} &= \widehat{C}_{\underline{31}} \cdot \left(\tfrac{8}{\pi^2 \cdot D_3^4}\right) \cdot |\dot{V}_T|^2 \cdot |\psi_3|^2 = \widehat{K}^{\dagger}_{\underline{31}} \cdot |\psi_3|^2 \end{aligned} \tag{B.1}$$

or using a general exponent m based on the Darcy's friction factor fitting (for details on m_{fit} see [2]), the power law becomes $m = (2 + m_{fit})$:

$$\begin{aligned} \widehat{\varphi}^{\dagger}_{\underline{31}} &= \widehat{C}_{\underline{31}} \cdot \left(\frac{8}{\pi^2 \cdot D_3^4}\right) \cdot \frac{|\dot{V}_T|^2}{|\psi_3|^{m_{fit}}} \cdot |\psi_3|^{(2+m_{fit})} \\ &= \widehat{K}_{\underline{31,fit}} \cdot |\psi_3|^{(2+m_{fit})} \end{aligned} \tag{B.2}$$

Notice that the value of $\widehat{K}^{\dagger}_{\underline{31}}$ or $\widehat{K}^{\dagger}_{\underline{31,fit}}$ in general, due to $\widehat{C}$, can be positive or negative in branched junctions, and therefore the sign of $\widehat{\varphi}^{\dagger}_{\underline{31}}$ is undefined.

Finally, it is easy to demonstrate that the same relationships (B.1) and (B.2) are valid, in general, for any fitting (see [2]).

B.2. Example of interacting branches

At the top of the Fig. B.7 the sizes and geometry of a round-duct example-network, are sketched, while at the bottom of the same figure we display the name assigned to each section and the work interaction at the branched junctions. Just, in the middle of the Fig. B.7, the elements of the flow model and their respective $\widehat{\varphi}^{\dagger}$

Table A.2
After the sizing step: pressure loss per section without including the diffuser and grilles

	Supply	Return	Return	Return	Return	Return
Name	I1	X1	X2	X3	X4	X5
Δp $[Pa]$	4.91	4.91	8.41	−4.13	8.40	−3.40

Table A.3
Comparison of the design and actual flow rates, at the diffuser and return grilles, for the sized network shown at the bottom of Fig. A.6.

Name	Design flow rate $[m^3/h]$	Actual flow $[m^3/h]$	v $[m/s]$	Δp $[Pa]$
D1	1600	1600	3.74	31.82
R2	1200	897	2.11	1.13
R1	200	414	2.34	7.80
R3	200	289	1.64	3.81

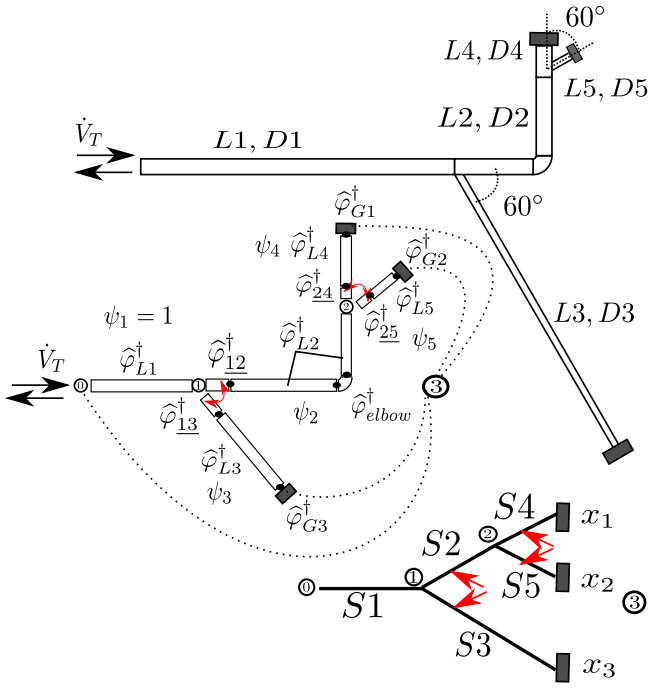

Fig. B.7. Example of a network to illustrate the MinEDP application. The middle scheme indicates the specific dissipation functions to be evaluated. The interacting branches are shown at the bottom.

are made explicit. Eq. (B.3) illustrates the concrete form of the global energy dissipation of this network. Notice that, by construction, $\widehat{\varphi}^{\dagger}_{L1}\cdot|\psi_1|$ is always constant, and that it is also always true that $\widehat{\varphi}=\widehat{\varphi}^{\dagger}$ but for the branched junctions. The global dissipation function is:

$$\begin{aligned}(F\circ h\circ g)(x_1,x_2) = \;& \widehat{\varphi}^{\dagger}_{L1}\cdot|\psi_1| + \left(\widehat{\varphi}^{\dagger}_{\underline{12}}+\widehat{\varphi}^{\dagger}_{L2}+\widehat{\varphi}^{\dagger}_{elbow}\right)\cdot|\psi_2| + \\ & \left(\widehat{\varphi}^{\dagger}_{\underline{13}}+\widehat{\varphi}^{\dagger}_{L3}+\widehat{\varphi}^{\dagger}_{G3}\right)\cdot|\psi_3| + \left(\widehat{\varphi}^{\dagger}_{\underline{24}}+\widehat{\varphi}^{\dagger}_{L4}+\widehat{\varphi}^{\dagger}_{G1}\right)\cdot|\psi_4| + \\ & \left(\widehat{\varphi}^{\dagger}_{\underline{25}}+\widehat{\varphi}^{\dagger}_{L5}+\widehat{\varphi}^{\dagger}_{G2}\right)\cdot|\psi_5| \\ (F\circ h\circ g)(x_1,x_2) = \;& \left[\widehat{\varphi}^{\dagger}\right]_1\cdot|\psi_1| + \left[\widehat{\varphi}^{\dagger}\right]_2\cdot|\psi_2| + \left[\widehat{\varphi}^{\dagger}\right]_3\cdot|\psi_3| + \left[\widehat{\varphi}^{\dagger}\right]_4\cdot|\psi_4| + \left[\widehat{\varphi}^{\dagger}\right]_5\cdot|\psi_5|\end{aligned} \tag{B.3}$$

If it is arbitrarily assumed that $m=2$ for the general potential law of Eq. (30) then Eq. (B.3) can be also written as:

$$\begin{aligned}(F\circ h\circ g)(x_1,x_2) = \;& \widehat{K}^{\dagger}_{L1}\cdot|\psi_1|^{(2+1)} + \overbrace{\left(\widehat{K}^{\dagger}_{\underline{12}}+\widehat{K}^{\dagger}_{L2}+\widehat{K}^{\dagger}_{elbow}\right)}^{\left[\widehat{K}^{\dagger}\right]_2}\cdot|\psi_2|^{(2+1)} + \\ & \left(\widehat{K}^{\dagger}_{\underline{13}}+\widehat{K}^{\dagger}_{L3}+\widehat{K}^{\dagger}_{G3}\right)\cdot|\psi_3|^{(2+1)} + \\ & \left(\widehat{K}^{\dagger}_{\underline{24}}+\widehat{K}^{\dagger}_{L4}+\widehat{K}^{\dagger}_{G1}\right)\cdot|\psi_4|^{(2+1)} + \\ & \left(\widehat{K}^{\dagger}_{\underline{25}}+\widehat{K}^{\dagger}_{L5}+\widehat{K}^{\dagger}_{G2}\right)\cdot|\psi_5|^{(2+1)}\end{aligned} \tag{B.4}$$

This latter assumption is made explicit, in Eq. (B.4), by writing the exponent as $(2+1)$. Recall that in the previous expression of F, the energy factors $\widehat{K}^{\dagger}$ are not necessarily constant. Additionally, their values also depend, on the exponent m chosen, but the global dissipation F is always the same for a certain flow distribution. A more compact way of writing (B.4) using the scalar product, is:

$$\begin{aligned}(F\circ h\circ g)(x_1,x_2) = \;& \left(\left[\widehat{K}^{\dagger}\right]_1,\left[\widehat{K}^{\dagger}\right]_2,\left[\widehat{K}^{\dagger}\right]_3,\left[\widehat{K}^{\dagger}\right]_4,\left[\widehat{K}^{\dagger}\right]_5\right)\cdot\left(|\psi_1|^3,|\psi_2|^3,|\psi_3|^3,|\psi_4|^3,|\psi_5|^3\right) \\ (F\circ h\circ g)(x_1,x_2) = \;& \overrightarrow{\widehat{K}^{\dagger}}\cdot\overrightarrow{|\psi|^3} = F(\vec{x})\end{aligned} \tag{B.5}$$

In Eq. (B.5), the symbols $\overrightarrow{\widehat{K}^{\dagger}}$ and $\overrightarrow{|\psi|^3}$ represent two vectors whose components are shown at the top of the same Eq. (B.5). Both depend, in general, on the independent variable $\vec{x}=(x_1,x_2)$. Finally, the "local" form of Eq. (B.4) is obtained by computing the energy factors at a certain test point or flow distribution, $\vec{x}_t$:

$$\begin{aligned}\left(\mathbb{F}|_{\vec{x}_t}\circ h\circ g\right)(x_1,x_2) = \;& \widehat{\mathbb{K}}^{\dagger}_{L1}|_{\vec{x}_t}\cdot|\psi_1|^{(2+1)} + \overbrace{\left(\widehat{\mathbb{K}}^{\dagger}_{\underline{12}}+\widehat{\mathbb{K}}^{\dagger}_{L2}+\widehat{\mathbb{K}}^{\dagger}_{elbow}\right)\Big|_{\vec{x}_t}}^{\left[\widehat{\mathbb{K}}^{\dagger}\right]_2|_{\vec{x}_t}}\cdot|\psi_2|^{(2+1)} + \\ & \left(\widehat{\mathbb{K}}^{\dagger}_{\underline{13}}+\widehat{\mathbb{K}}^{\dagger}_{L3}+\widehat{\mathbb{K}}^{\dagger}_{G3}\right)\Big|_{\vec{x}_t}\cdot|\psi_3|^{(2+1)} + \\ & \left(\widehat{\mathbb{K}}^{\dagger}_{\underline{24}}+\widehat{\mathbb{K}}^{\dagger}_{L4}+\widehat{\mathbb{K}}^{\dagger}_{G1}\right)\Big|_{\vec{x}_t}\cdot|\psi_4|^{(2+1)} + \\ & \left(\widehat{\mathbb{K}}^{\dagger}_{\underline{25}}+\widehat{\mathbb{K}}^{\dagger}_{L5}+\widehat{\mathbb{K}}^{\dagger}_{G2}\right)\Big|_{\vec{x}_t}\cdot|\psi_5|^{(2+1)} = \mathbb{F}|_{\vec{x}_t}(x_1,x_2)\end{aligned} \tag{B.6}$$

The evaluation of the component $\left[\widehat{K}^{\dagger}\right]_2$ at some test point $\vec{x}_t$ is written as $\left[\widehat{\mathbb{K}}^{\dagger}\right]_2|_{\vec{x}_t}$. Recall that Eq. (B.6), when there exist work interaction, is not strictly a *pure* dissipation function.

According to our previous paper [2], for $m=2$ the energy (dissipation) factor of a straight i-conduit is given by:

$$\widehat{\varphi}^{\dagger}_{Li} = \overbrace{f_{D,i}\cdot\left(\frac{8\rho L}{\pi^2\cdot D^5}\right)}^{\widehat{K}^{\dagger}_{Li}}\cdot|\dot{V}_T|^2\cdot|\psi_i|^2, \tag{B.7}$$

while for any branched junction $\widehat{K}^{\dagger}_{\underline{\_\_}}$, elbow-fitting $\widehat{K}^{\dagger}_{elbow}$ and any grille $\widehat{K}^{\dagger}_{G-}$ the Eq. (B.1), can be used to define the energy factor. This latter Eq. (B.1), in turn, is based on the head *change* coefficient C of the branched junction, the elbow and the grilles. Just for illustrative purposes, four network cases, based on the example of Fig. B.7 have been analyzed, operating either in supply (s) or return (r) mode. In all cases, the head *change* coefficient of the elbow fitting is $C=0.22$. The total flow rate $\dot{V}_T$ has been kept constant and it is imposed either as supply or return flow. Although the effective head *change* C at a certain given grille, is different in supply and return modes, here their values have been kept constant for all cases. Therefore, the only difference between supply and return operating modes, in our example, has been the selection of the energy factor (ultimately, the head *change* coefficient) for the branched junctions. This dependence of the energy factor on the sense of the flow, for non-symmetrical elements, must be taken into account, implicitly, by the procedure. As aforementioned, the grilles head loss is also non-symmetrical but their values were kept constant in all cases, so that, in practice, it is like having two different types of grilles: one for supply and another for return mode.

Table B.4
Example return network. Summary of the different cases.

Case	Geometry	Return grilles C
#1(s) (r)	$\vec{L} = (10, 5, 10, 1, 1)$ $\vec{D} = (0.50, 0.50, 0.45, 0.50, 0.45)$	0.1
#2(s) (r)	same as case 1	1.0
#3(s) (r)	$\vec{L} = (10, 5, 10, 1, 1)$ $\vec{D} = (0.50, 0.50, 0.20, 0.50, 0.20)$	1.0
#4(s) (r)	$\vec{L} = (10, 5, 10, 1, 1)$ $\vec{D} = (0.50, 0.50, 0.50, 0.50, 0.50)$	1.0

The head *change* coefficients of the branched junctions have been obtained from Idelchik [22].[5] The, Eqs. (B.8) and (B.9), show their expressions but using our nomenclature instead of the Idelchik's guidebook.

$$C_{31} = \frac{\widehat{\varphi}^{\dagger}_{31}}{\rho \bar{v}_1^2/2} = 1 - \left(1 - \frac{\dot{V}_2}{\dot{V}_1}\right)^2 - \frac{A_1}{A_2}\left(\frac{\dot{V}_2}{\dot{V}_1}\right)^2 \tag{B.8a}$$

$$C_{21} = \frac{\widehat{\varphi}^{\dagger}_{21}}{\rho \bar{v}_1^2/2} = a \cdot \left[1 + \left(\frac{\dot{V}_2}{\dot{V}_1}\frac{A_1}{A_2}\right)^2 - 2\left(1 - \frac{\dot{V}_2}{\dot{V}_1}\right)^2 - \frac{A_1}{A_2}\left(\frac{\dot{V}_2}{\dot{V}_1}\right)^2\right] \tag{B.8b}$$

$$a = \begin{cases} \text{if} A_2/A_1 \leqslant 0.35 \text{then} 1 \text{otherwise} 0 \\ \text{else} \\ \text{if} \dot{V}_2/\dot{V}_1 \leqslant 0.4 \text{then} 0.9 \cdot \left(1 - \dot{V}_2/\dot{V}_1\right) \\ \text{else} 0.55 \end{cases} \tag{B.8c}$$

Eq. (B.8) Convergent $60^{\circ}, A_2 + A_3 > A_1, A_1 = A_3$ (Idelchik [22])

$$C_{12} = \frac{\widehat{\varphi}^{\dagger}_{12}}{\rho \bar{v}_1^2/2} = a' \cdot \left[1 + \left(\frac{\dot{V}_2/\dot{V}_1}{A_2/A_2}\right)^2 - 2\frac{\dot{V}_2/\dot{V}_1}{A_2/A_2} \cdot \cos\alpha\right] \tag{B.9a}$$

$$C_{13} = \frac{\widehat{\varphi}^{\dagger}_{13}}{\rho \bar{v}_1^2/2} = 0.4 \cdot \left(\dot{V}_2/\dot{V}_1\right)^2 \tag{B.9b}$$

$$a' = \begin{cases} \text{if } A_2/A_1 \leqslant 0.35 \text{then if} \dot{V}_2/\dot{V}_1 \leqslant 0.4 \text{then} 1.1 - 0.7 \cdot \dot{V}_2/\dot{V}_1 \text{ else } 0.85 \\ \text{else} \\ \text{if } \dot{V}_2/\dot{V}_1 \leqslant 0.6 \text{then} 1.1 - 0.65 \cdot \dot{V}_2/\dot{V}_1 \text{ else } 0.60 \end{cases} \tag{B.9c}$$

(B.9) Divergent $0 < \alpha \leqslant 60^{\circ}, A_2 + A_3 > A_1, A_1 = A_3$ (Idelchik [22]).

In every case the starting iteration point was the same $\vec{x}_0 : x_1 = 0.5$ and $x_2 = 0.4$. However a series of runs, with the initial point chosen arbitrarily, were also performed without problems of convergence or appreciable changes in calculation speed.

Table B.4 shows the geometry for each case and the C of the grilles. The lengths and angles of the network sections are kept constant but, depending on the case, the diameters change (see sections $\{3, 4, 5\}$ in that table).

The properties of the air at 20 $[^{\circ}C]$ and 1$[bar]$ are assumed to be: $\nu = 1.813 \cdot 10^{-5}$ $\left[kg \cdot s^{-1} \cdot m^{-1}\right], 1/\rho = 0.85$ $\left[m^3/kg\right]$. The roughness of the duct corresponds to galvanized steel sheet $\epsilon = 0.14$. As mentioned, section $S1$ has always the same values: $\dot{V}_1 = \dot{V}_T = 1.374450$ $[m^3/s]$ or $\psi_1 = 1$, $Re = 234288$, $\nu = 7.00$ $[m/s]$, $\epsilon/D = 0.28$, either operating in supply or return mode.

Tables B.5 and B.6 show the results of a total of eight runs: four cases times two modes. In Table B.5, cases #1 and #2 compare the effect of just increasing the C at the grilles. Looking at the column named ψ, the flow rate ratio in each network section can be compared. Notice its big impact on the flow distribution, reaching even a case where in section $S5$ the supply flow is practically zero. In Table B.6, cases #3 and #4 compare the effect of increasing the diameter of sections $S3$ and $S5$. It can be checked that the effect is very different in supply and return modes.

Nevertheless, our goal here is to illustrate the new method and to verify that it copes with the difficulties posed at Section 1. As aforementioned, despite the very different flow distribution at the solution for each case, the new method worked very well. Regardless of the initial point $\vec{x}_0$, the method was always robust in finding the solution.

In order to visualize the ideas and concepts of the new method, the Fig. B.8 has been included. It represents the actual values for the case $\#2(r)$ (the return mode). The (x_1, x_2) plane represents different flow distributions and the $z - axis$ represents different specific power functions per unit of total volume flow rate $[Pa]$. It only has the meaning of an actual power dissipation for the F function. Two, of the represented surfaces, correspond to functions already presented in the paper: the global dissipation function $F(x_1, x_2)$ (or the actual dissipation) and a "local" function $\mathbb{F}(x_1, x_2)$ computed at the test point $\vec{x}_t = (0.35, 0.35)$. It is worthwhile to stress that: $F(\vec{x})$ is an hypothetical energy dissipation of the network, or in other words, $F(\vec{x}_t)$ would be the dissipated power per unit of $\dot{V}_T$, if the network could be kept at the flow distribution $\vec{x}_t$ but actually, this is not physically possible. Moreover, any point on the F surface has a net *external* work equal to zero, i.e., all work interactions are internal and cancel out. On the other hand, $\mathbb{F}|_{\vec{x}_t}$, would be the local energy "dissipation" (warning: see Section 2.5 for details), of the network, if the physical mechanisms of dissipation and work exchange were "frozen" at the values that the flow distribution really has at the test point $\vec{x}_t$ (i.e. $\widehat{K}^{\dagger}$ are kept constant for those conditions). This makes a great difference. It means that any point on the surface $\mathbb{F}|_{\vec{x}_t}$ has a net *external* work exchanged *not* equal to zero, although it looks similar to F. The only point on that surface, where the work cancels out is, by definition, on the test point $\vec{x}_t$. The third function in Fig. B.8, is an auxiliary function $F_{aux}(x_1, x_2)$ whose goal is to visualize that the solution $\vec{x}_{sol}$ is not at the minimum of the global dissipation function $F(\vec{x}_{sol}) \neq F_{min}$. The new function is defined as follows: to any test point $\vec{x}_t$ the mapped value $F_{aux}(\vec{x}_t)$, is computed as the minimization of the "local" form $\mathbb{F}|_{\vec{x}_t}$, i.e. $F_{aux}(\vec{x}_t) = \text{minimum}_{\vec{x}}\left(\mathbb{F}|_{\vec{x}_t}(\vec{x})\right)$ (see Fig. B.8). According to the discussion in Section 2.5, this auxiliary function satisfies an interesting property: it should touch the global dissipation function at a single point, since if $\vec{x}_t = \vec{x}_{sol}$ then $F_{aux}(\vec{x}_{sol}) = \text{minimum}_{\vec{x}}\left(\mathbb{F}|_{\vec{x}_{sol}}(\vec{x})\right) = F(\vec{x}_{sol})$ which are precisely the conditions for being a solution of the steady-state flow distribution, otherwise $F_{aux}(\vec{x}_t) \neq F(\vec{x}_t)$, i.e., they have no points in common.

Using the Fig. B.8, the solution procedure can be visualized. At the flow distribution plane (x_1, x_2) three iteration steps are displayed. Let's have a look at the two final ones. The iteration is at $\vec{x}_t$, and after computing the $\widehat{K}^{\dagger}$ factors to create the "local" form $\mathbb{F}|_{\vec{x}_t}(\vec{x})$, this function is minimized leading practically to the solution $\vec{x}_{sol}$. Now, since $\vec{x}_{sol}$ is not coherent or compatible with the previous physics assumed in $\mathbb{F}$, a new compatible vector with $\left[\widehat{K}^{\dagger}_{sol}\right]$ components is computed at $\vec{x}_{sol}$, and a new "local" form $\mathbb{F}|_{\vec{x}_{sol}}(\vec{x})$ is obtained (warning: the surface $\mathbb{F}|_{\vec{x}_{sol}}(\vec{x})$ is not shown in the Fig. B.8). This new "local" form has a minimum at $\vec{x}_{sol'}$ and therefore within a certain tolerance: $\vec{x}_{sol} \approx \vec{x}_{sol'}$ or $\overrightarrow{\widehat{K}}^{\dagger}_{sol} \approx \overrightarrow{\widehat{K}}^{\dagger}_{sol'}$ and the solution is reached.

On the top right of Fig. B.8, there is a side-view of the three surfaces. There it can be seen clearly that the F_{aux} touches the global dissipation at a single point, close to its minimum but not at the minimum of $F(\vec{x})$. One outcome, from this fact, is a better understanding of why a small modification of the resistance of the net-

[5] These coefficients may change, due to recent revision, with the edition of the Idelchik guidebook, here they are taken as valid for illustrative purposes.

Table B.5
Cases #1 and #2. Results for the example shown in Fig. B.7. Effect of the loss at the grilles. Note: (r) return, (s) supply.

Case parameters	Case Number	$\Delta p_T[Pa]$	Power $[W]$	x_1	x_2
$C_{gr} = 0.1$	#1(r)	159.633	219.407	0.2909160	0.3031394
$D_3 = D_5 = 0.45[m]$	#1(s)	157.783	216.865	0.6986250	≈ 0
Section	ψ	$\dot{V}[m^3/s]$	Reynolds	$v[m/s]$	ϵ/D
S2(r)	0.594	0.816498	139180	4.16	0.28
S2(s)	0.699	0.960223	163679	4.89	
S3(r)	0.406	0.557949	105676	3.51	0.31
S3(s)	0.301	0.414224	78453	2.60	
S4(r) 4(s)	0.291	0.399849	68158	2.04	0.28
	0.699	0.960223	163679	4.89	
S5(r)	0.303	0.416649	78913	2.62	0.31
S5(s)	0.000	≈ 0	≈ 0	≈ 0	
Case parameters	Case Number	$\Delta p_T[Pa]$	Power $[W]$	x_1	x_2
$C_{gr} = 1.0$	#2(r)	163.472	224.683	0.3130019	0.2921281
$D_3 = D_5 = 0.45[m]$	#2(s)	162.314	223.092	0.5381383	0.1541103
Section	ψ	$\dot{V}[m^3/s]$	Reynolds	$v[m/s]$	ϵ/D
S2(r)	0.605	0.831719	141775	4.24	0.28
S2(s)	0.692	0.951459	162186	4.85	
S3(r)	0.395	0.542728	102793	3.41	0.31
S3(s)	0.308	0.422988	80113	2.66	
S4(r)	0.313	0.430204	73332	2.19	0.28
S4(s)	0.538	0.739642	126079	3.77	
S5(r)	0.292	0.401514	76046	2.52	0.31
S5(s)	0.154	0.211816	40118	1.33	

Table B.6
Cases #3 and #4. Results for the example shown in Fig. B.7. Effect of the diameter of the side branches. Note: (r) return, (s) supply.

Case parameters	Case Number	$\Delta p_T[Pa]$	Power $[W]$	x_1	x_2
$C_{gr} = 1.0$	#3(r)	210.389	289.168	0.8386228	0.0991515
$D_3 = D_5 = 0.20[m]$	#3(s)	209.344	287.733	0.8882054	0.0623936
Section	ψ	$\dot{V}[m^3/s]$	Reynolds	$v[m/s]$	ϵ/D
S2(r)	0.938	1.288920	219709	6.56	0.28
S2(s)	0.951	1.306550	222714	6.65	0.28
S3(r)	0.062	0.085526	36446	2.72	0.70
S3(s)	0.049	0.067899	28935	2.16	0.70
S4(r)	0.839	1.152640	196479	5.87	0.28
S4(s)	0.888	1.220790	208096	6.22	0.28
S5(r)	0.099	0.136278	58075	4.34	0.70
S5(s)	0.062	0.085756	36545	2.73	0.70
Case parameters	Case Number	$\Delta p_T[Pa]$	Power $[W]$	x_1	x_2
$C_{gr} = 1.0$	#4(r)	157.161	216.009	0.2351134	0.2956164
$D_3 = D_5 = 0.50[m]$	#4(s)	156.764	215.464	0.5001686	0.1431726
Section	ψ	$\dot{V}[m^3/s]$	Reynolds	$v[m/s]$	ϵ/D
S2(r)	0.531	0.729460	124344	3.72	0.28
S2(s)	0.643	0.884238	150727	4.5	0.28
S3(r)	0.469	0.644987	109944	3.29	0.28
S3(s)	0.357	0.490208	83561	2.5	0.28
S4(r)	0.235	0.323151	55084	1.65	0.28
S4(s)	0.500	0.687455	117184	3.5	0.28
S5(r)	0.296	0.406309	69259	2.07	0.28
S5(s)	0.143	0.196783	33544	1.0	0.28

work (or the global dissipation function) may produce a quite big change in the flow distribution without hardly changing the dissipated power of the network. An example of this, can be found by looking at cases $\#3(r)$ and $\#4(r)$, in Table B.6.

The paper presents the main outcomes and ideas about the application of MinEDP for solving the steady-state flow distribution of general networks. Therefore, a detailed study of the computational performance is out of the scope, since no optimization has been studied. However, as a reference, we can provide some data. The method was implemented in Scilab. The minimization method for $\mathbb{F}$ was the Nelder-Meads algorithm. The tolerance in the search space was 10^{-9} and was applied to the no rm of the vector $\overrightarrow{\widetilde{K}}^{\dagger}$. The convergence of the overall fixed point problem and minimization steps, was very fast. In regard to convergence, the value of m has an effect which deserves to be studied a bit further. The physical meaning of the exponent m in the potential law (22) is discussed in [2]. As mentioned here and explained in [2], the exact value of m does not really matter to reach the solution. As it has been shown the energy dissipation and the internal work interactions determine the solution. The exponent m acts as a tunning parameter for the measure of the dissipation/interaction power. In a preliminary check, the number of iterations does depend on the m (see [2]). For instance, in a network without work interactions and made up only of smooth straight conduits m can be chosen so that in a single minimization step the solution is found (see [2]).

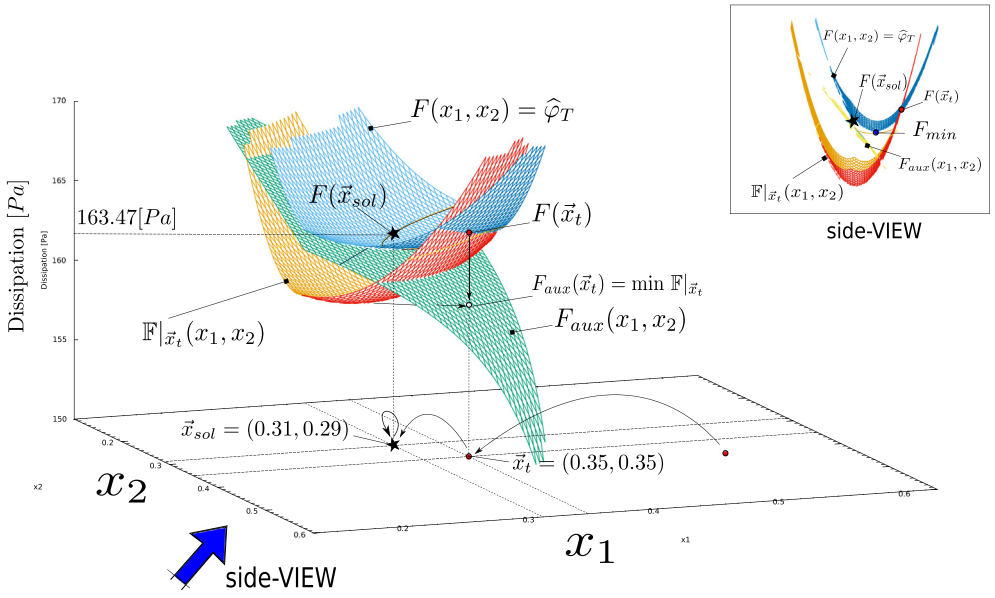

Fig. B.8. Case $\#2(r)$: actual representation in $\vec{x} \times$ Dissipation space of several dissipation surfaces defined in the paper. The flow distribution solution is marked with a ☆. The side-view illustrates that the solution is not at the minimum of the global dissipation function F.

References

[1] B. Schmandt, H. Herwig, The head change coefficient for branched flows: Why losses due to junctions can be negative, International Journal of Heat and Fluid Flow 54 (2015) 268–275, https://doi.org/10.1016/j.ijheatfluidflow.2015.06.004, URL: http://www.sciencedirect.com/science/article/pii/S0142727X15000697.

[2] V.-M. Soto-Frances, J.-M. Pinazo-Ojer, E.-J. Sarabia-Escriva, P.-J. Martinez-Beltran, On using the minimum energy dissipation to estimate the steady-state of a flow network and discussion about the resulting power-law: application to tree-shaped networks in hvac systems, Energy 172 (2019) 181–195, https://doi.org/10.1016/j.energy.2019.01.060, URL: https://www.sciencedirect.com/science/article/pii/S0360544219300623.

[3] M. Podfigurna, approved by board of directors, Applying energy efficient measures for metal and metalworking SMEs and industry, URL: https://cordis.europa.eu/project/id/694638/reporting (Feb. 2019)..

[4] S.A. Saravia, P.C. Raynor, A.J. Streifel, A performance assessment of airborne infection isolation rooms, American Journal of Infection Control 35 (2007) 324–331, https://doi.org/10.1016/j.ajic.2006.10.012.

[5] G. Xu, C.T. Yang, L. Zhao, Minimum Energy Dissipation Rate Theory and Its Applications for Water Resources Engineering, Springer International Publishing, Cham, 2015, pp. 183–245, https://doi.org/10.1007/978-3-319-11023-3_5, URL: https://doi.org/10.1007/978-3-319-11023-3_5.

[6] V.-M. Soto-Frances, J. manuel Pinazo-Ojer, E.-J. Sarabia-Escriva, P.-J. Martinez-Beltran, About using the minimum energy dissipation to find the steady-state flow distribution in networks, URL: https://advanceseng.com/new-pipe-network-analysis-method-minimum-energy-dissipation-principle-application-tree-shaped-duct-networks-hvac-systems/, presented at Heat Transfer, Fluid Mechanics and Thermodynamics, 14th international conference. HEFAT, Wicklow Ireland. (2019)..

[7] E.A. Meulman, A pipe flow network model with incorporation of a junction pressure loss model, Master's thesis, Delft University of Technology. Electrical Engineering, Mathematics and Computer Science, Applied Sciences, bachelor Thesis (July 5 2016)..

[8] J. Štigler, Tee junction as a pipeline net element. Part 1 a new mathematical model, Strojncky casopis 57 (5) (2006) 249–262, iSSN: 0039-2472..

[9] J.E.F. Don, J. Wood, L. Srinivasa Reddy, Modeling pipe networks dominated by junctions, Journal of Hydraulic Engineering 119 (8) (1993) 949–958.

[10] J.A. Liggett, Discussion: Modeling pipe networks dominated by junctions, Journal of Hydraulic Engineering 120 (12) (1993) 1486–1489.

[11] J.E.F. Don J. Wood, L. Srinivasa Reddy, Clousure on: Modeling pipe networks dominated by junctions, Journal of Hydraulic Engineering 120 (12) 1492–1493..

[12] J. Štigler, Tee junction as a pipeline net element. Part 2. coefficients determination, Strojncky asopis 57 (5) (2006) 263–270, iSSN: 0039-2472..

[13] H.M.H. Donald, C. Rennels, Pipe Flow. A Practical and Comprehensive Guide, John Wiley & Sons Inc., Hoboken, New Jersey, 2012, iSBN 978-0-470-90102-1..

[14] B.L.C.A.S. Ramamurthy, Weimin Zhu, Dividing rectangular closed conduit flows, Journal of Hydraulic Engineering 122 (12) (1996) 687–691.

[15] Q. Wang, Y. Pan, M. Zhu, Z. Huang, P. Xu, A new local pressure loss coefficient model of a duct tee junction applied during transient simulation of a hvac air-side system, Journal of Building Performance Simulation 11 (1) (2018) 113–127. arXiv:https://doi.org/10.1080/19401493.2017.1288762, doi:10.1080/19401493.2017.1288762. URL: https://doi.org/10.1080/19401493.2017.1288762..

[16] M.T. Vladan, D. Dordević, Vladimir Raičević, A new approach to the evaluation of friction and separation losses in ducts, Facta Universitatis 2 (7/2) (1997) 341–352, URL: http://facta.junis.ni.ac.rs/macar/macar97s/macar97s-02.pdf.

[17] S.B.R. Guohui Gan, Numerical determination of energy losses at duct junctions, Applied Energy 67 (2000) 331–340.

[18] B.S. Heinz Herwig, Drag with external and pressure drop with internal flows: a new and unifying look at losses in the flow field based on the second law of thermodynamics, Fluids Dynamics Research 45, doi:10.1088/0169-5983/45/5/055507..

[19] H. Herwig, B. Schmandt, How to determine losses in a flow field: A paradigm shift towards the second law analysis, Entropy 16 (6) (2014) 2959–2989, https://doi.org/10.3390/e16062959, URL: http://www.mdpi.com/1099-4300/16/6/2959.

[20] H.H. Bastian Schmandt, Losses due to the flow through conduit components in mini- and micro- systems accounted for by head loss/change coefficients, in: Proceedings of the ASME 2014 4th Joint US-European Fluids Engineering Division Summer Meeting and 12th International Conference on Nanochannels, Microchannels, and Minichannels,Chicago, Illinois, USA, ASME, 2014.

[21] E. Mathews, D. Claassen, Problems with the t-method, Building and Environment 33 (4) (1998) 173–179, https://doi.org/10.1016/S0360-1323(97)00033-4, URL: https://www.sciencedirect.com/science/article/pii/S0360132397000334.

[22] I.E. Idelchik, Handbook of hydraulic resistance (2nd Edition), Hemisphere Publishing Corporation, 1986, ISBN: 0-89116-284-4..

[23] L. Tong, J. Gao, Z. Luo, L. Wu, L. Zeng, G. Liu, Y. Wang, A novel flow-guide device for uniform exhaust in a central air exhaust ventilation system, Building and Environment 149 (2019) 134–145, https://doi.org/10.1016/j.buildenv.2018.12.007, URL: https://www.sciencedirect.com/science/article/pii/S036013231830742X.